

**REMOVAL OF TRACE OLEFINS FROM AROMATICS WITH MODIFIED  
USY ZEOLITE AND CLAYS**

Sirawit Lertprapaporn

A Thesis Submitted in Partial Fulfillment of the Requirements  
for the Degree of Master of Science  
The Petroleum and Petrochemical College, Chulalongkorn University  
in Academic Partnership with  
The University of Michigan, The University of Oklahoma,  
Case Western Reserve University, and Institut Français du Pétrole  
2020

บทคัดย่อและแฟ้มข้อมูลฉบับเต็มของวิทยานิพนธ์ตั้งแต่ปีการศึกษา 2554 ที่ให้บริการในคลังปัญญาจุฬาฯ (CUAIR)

เป็นแฟ้มข้อมูลของนิสิตเจ้าของวิทยานิพนธ์ที่ส่งผ่านทางบัณฑิตวิทยาลัย

The abstract and full text of theses from the academic year 2011 in Chulalongkorn University Intellectual Repository (CUAIR)  
are the thesis authors' files submitted through the Graduate School.

3872731635



CU iThesis 6171022063 thesis / recv: 20072563 15:54:37 / seq: 19



3872731635

# Removal of Trace Olefins from Aromatics with Modified USY Zeolite and Clays

Mr. Sirawit Lertpraporn

A Thesis Submitted in Partial Fulfillment of the Requirements  
for the Degree of Master of Science in Petrochemical Technology  
Common Course  
the Petroleum and Petrochemical College  
Chulalongkorn University  
Academic Year 2019  
Copyright of Chulalongkorn University



3872731635

CU ThesIs 6171022063 thesis / recv: 20072563 15:54:37 / seq: 19

การกำจัดโอเลฟินส์จากอะโรมาติกด้วยตัวเร่งปฏิกิริยาซีโอไลต์ชนิดยูเอสวายและเคลย์ที่ผ่านการ  
ดัดแปลง

นายสิริวิชญ์ เลิศประภาภรณ์

วิทยานิพนธ์นี้เป็นส่วนหนึ่งของการศึกษาตามหลักสูตรปริญญาวิทยาศาสตรมหาบัณฑิต  
สาขาวิชาเทคโนโลยีปิโตรเคมี ไม่สังกัดภาควิชา/...  
วิทยาลัยปิโตรเลียมและปิโตรเคมี จุฬาลงกรณ์มหาวิทยาลัย  
ปีการศึกษา 2562  
ลิขสิทธิ์ของจุฬาลงกรณ์มหาวิทยาลัย



3872731635

CU Thesisis 6171022063 thesis / recv: 20072563 15:54:37 / seq: 19

Thesis Title                      Removal of Trace Olefins from Aromatics with  
Modified USY Zeolite and Clays  
By                                      Mr. Sirawit Lertpraporn  
Field of Study                      Petrochemical Technology  
Thesis Advisor                      Professor PRAMOCH RANGSUNVIGIT, Ph.D.  
Thesis Co Advisor                      Professor BOONYARACH KITIYANAN, Ph.D.

---

Accepted by the the Petroleum and Petrochemical College, Chulalongkorn  
University in Partial Fulfillment of the Requirement for the Master of Science

..... Dean of the the Petroleum and  
Petrochemical College  
(Professor SUWABUN CHIRACHANCHAI, Ph.D.)

#### THESIS COMMITTEE

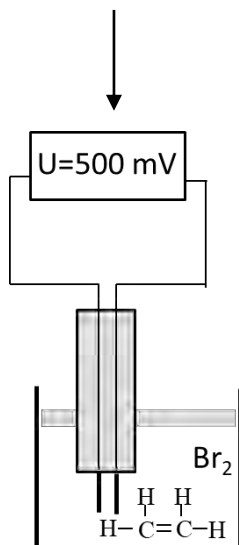
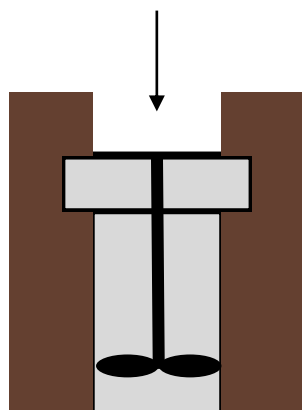
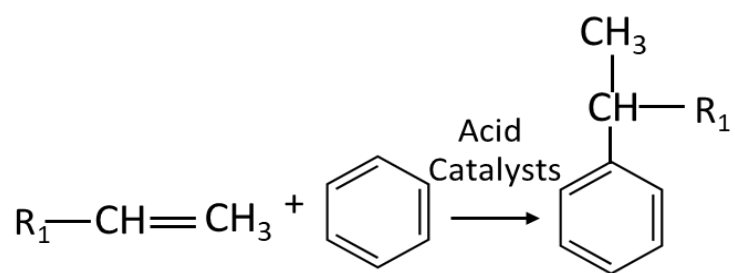
..... Chairman  
(Assistant Professor UTHAIPORN  
SURIYAPRAPHADILOK, Ph.D.)  
..... Thesis Advisor  
(Professor PRAMOCH RANGSUNVIGIT, Ph.D.)  
..... Thesis Co-Advisor  
(Professor BOONYARACH KITIYANAN, Ph.D.)  
..... External Examiner  
(Pathamaporn Wattanaphan, Ph.D.)



3872731635

CD IThesis 6171022063 thesis / recv: 20072563 15:54:37 / seq: 19

# GRAPHICAL ABSTRACT



3872731635

CU iThesis 6171022063 thesis / recv: 20072563 15:54:37 / seq: 19

สิริวิษณุ เลิศประภากรณ์ : การกำจัดโอเลฟินส์จากอะโรมาติกด้วยตัวเร่งปฏิกิริยาซีโอไลต์ชนิดยูเอสวายและเคลย์ที่ผ่านการดัดแปลง. ( Removal of Trace Olefins from Aromatics with Modified USY Zeolite and Clays) อ.ที่ปรึกษาหลัก : ศ. ดร.ปราโมช รังสรรค์วิจิตร, อ.ที่ปรึกษาร่วม : ศ. ดร.บุญยรัชต์ กิตติยานันท์

รีฟอร์มเมตจากอุตสาหกรรมกลั่นน้ำมันเป็นสารตั้งต้นที่สำคัญในอุตสาหกรรมปิโตรเคมี ซึ่งรีฟอร์มเมตนี้ประกอบไปด้วยสารในกลุ่มอะโรมาติกไฮโดรคาร์บอนเป็นองค์ประกอบหลักและสารในกลุ่มของโอเลฟินส์ที่เป็นสารปนเปื้อน เนื่องจากโอเลฟินส์ทำอันตรายกับสารดูดซับในกระบวนการผลิตในขั้นต่อไปจึงต้องกำจัดโอเลฟินส์ก่อนส่งไปยังอุตสาหกรรมปิโตรเคมี การกำจัดโอเลฟินส์ทำได้โดยปฏิกิริยาแอลคิลเลชั่นซึ่งเป็นปฏิกิริยาที่สารในกลุ่มอะโรมาติกทำปฏิกิริยากับโอเลฟินส์โดยมีผลิตภัณฑ์เป็นแอลคิลอะโรมาติกโดยใช้ตัวเร่งปฏิกิริยาชนิดกรด ในงานวิจัยนี้จึงคัดเลือกเคลย์และซีโอไลต์ชนิดต่างๆ ที่เหมาะสมกับปฏิกิริยานี้มาดัดแปลงเพื่อเพิ่มประสิทธิภาพของการกำจัดโอเลฟินส์ให้สูงขึ้น การทดลองนี้ดำเนินการในเครื่องปฏิกรณ์แบบกะใช้เวลา 6 ชั่วโมงที่อุณหภูมิ 195 องศาเซลเซียส และความดัน 12 บาร์ โดยซีโอไลต์ชนิดยูเอสวายผ่านการดัดแปลงด้วยวิธีการคืออุมิเนชั่นด้วยกรดซัลฟิวริกที่ความเข้มข้น 0.075 ถึง 0.3 โมลลาร์ ส่วนเคลย์ชนิดเบนโทไนท์ผ่านการดัดแปลงด้วยวิธีการชะล้างด้วยกรดไฮโดรคลอริกที่ความเข้มข้น 1 ถึง 6 โมลลาร์ ทั้งนี้ได้วิเคราะห์ตัวเร่งปฏิกิริยาทั้งหมดผ่านเครื่องวิเคราะห์การเลี้ยวเบนของรังสีเอกซ์ เครื่องวิเคราะห์ธาตุด้วยการเรืองรังสีเอกซ์ เครื่องวัดพื้นที่ผิวและความพรุน เครื่องวิเคราะห์การคายซับโดยใช้อุณหภูมิ และเครื่องวิเคราะห์ทางความร้อน โดยผลจากการศึกษาพบว่า ซีโอไลต์ชนิดยูเอสวายดัดแปลงด้วยกรดซัลฟิวริกความเข้มข้น 0.15 โมลลาร์ มีพื้นที่ผิวสูงขึ้นและสัดส่วนของกรดแก่ที่เหมาะสมทำให้ความสามารถในการกำจัดโอเลฟินส์ในช่วงดันเพิ่มจาก 76% ไป 87% และเพิ่มความสามารถในการกำจัดโอเลฟินส์ในช่วงท้ายจาก 84% ไป 90% ในทำนองเดียวกันเคลย์ชนิดเบนโทไนท์ดัดแปลงด้วยกรดไฮโดรคลอริกความเข้มข้น 1 โมลลาร์ สามารถเพิ่มความเป็นกรดของเบนโทไนท์ส่งผลให้เพิ่มความสามารถในการกำจัดโอเลฟินส์ในช่วงดันเพิ่มจาก 74% ไป 81% และเพิ่มความสามารถในการกำจัดโอเลฟินส์ในช่วงท้ายจาก 86% ไป 90%

สาขาวิชา เทคโนโลยีปิโตรเคมี

ลายมือชื่อนิติ

ปีการศึกษา 2562

ลายมือชื่อ อ.ที่ปรึกษาหลัก

ลายมือชื่อ อ.ที่ปรึกษาร่วม



3872731635

## 6171022063 : MAJOR PETROCHEMICAL TECHNOLOGY

KEYWORD Aromatics/ Alkylation/ Acid activation/ Bentonite/ Dealumination/  
D: Olefins / USY

Sirawit Lertpraporn : Removal of Trace Olefins from Aromatics with Modified USY Zeolite and Clays. Advisor: Prof. PRAMOCH RANGSUNVIGIT, Ph.D. Co-advisor: Prof. BOONYARACH KITIYANAN, Ph.D.

Naphtha reforming is an important raw material for aromatic hydrocarbon products in petrochemical processes. However, aromatic hydrocarbon streams obtained from refinery contain unavoidable trace amounts of olefins as an impurity. The trace olefins must be removed because these undesirable olefins are harmful to the following separation processes. Alkylation reaction has been used to remove olefins with acid catalysts. In this study, clays and zeolites were screened for further modification in order to enhance the catalytic activity of olefins removal. The catalytic activity testing was studied in a batch reactor at 195 °C for 6 h under 12 barg. USY was modified by dealumination with 0.075 – 0.3 M citric acid, and bentonite was modified by acid activation with 1 – 6 M hydrochloric acid. The properties of catalysts were determined by XRD, XRF, N<sub>2</sub> adsorption, TPD-NH<sub>3</sub>, and STA. The results showed that the modification of USY with 0.15 M citric acid increased the surface area and proportion of strong acid sites to total acid sites resulting in the increase in the initial and final olefins removal from 76 to 87% and 84 to 90%, respectively. Likewise, the modification of bentonite with 1 M hydrochloric acid increased the acidity leading to the increase in the initial and final olefins removal from 74 to 81% and 86 to 90%, respectively.

|                 |                          |                                 |
|-----------------|--------------------------|---------------------------------|
| Field of Study: | Petrochemical Technology | Student's Signature<br>.....    |
| Academic Year:  | 2019                     | Advisor's Signature<br>.....    |
|                 |                          | Co-advisor's Signature<br>..... |

## ACKNOWLEDGEMENTS

I would like to express my gratitude to all who gave me to complete this thesis. First of all, I would like to sincerely thank my thesis advisor and co-advisor, Prof. Pramoch Rangsunvigit and Prof. Boonyarach Kitiyanan, for their patient guidance, understanding, and constant encouragement throughout of this work. Their positive attitude contributed significantly to inspire and maintain my enthusiasm in this field. I will always be proud to have been their student. I would like to thank Asst.Prof. Uthaiporn Suriyaphradilok and Dr. Pathamaporn Wattanaphan for their kind advice and for being the thesis committee. I also would like to thank all of my professors at the Petroleum and Petrochemical College for their generous help.

The authors would like to acknowledge the PPC 30 years 30 scholarships granted by Thai Oil Public Company Limited and the Petroleum and Petrochemical College. I would like to thank Dr. Yindee Suttisawat from Thai Oil Public Company Limited for guidance, suggestion, and support.

Special appreciation goes to all of the Petroleum and Petrochemical College's staff who gave me helps in various aspects, especially the research affairs staff who kindly help with the analytical instrument used in this work.

Finally, I would like to give my special thank to my family for a long time your supported me to study. In addition, I would like to thank all of my friends for their friendly help, creative suggestion, and encouragement.

Sirawit Lertprapaporn



# TABLE OF CONTENTS

|  | <b>Page</b> |
|--|-------------|
| ABSTRACT (THAI) .....  | iii         |
| ABSTRACT (ENGLISH).....  | iv          |
| ACKNOWLEDGEMENTS.....  | v           |
| TABLE OF CONTENTS.....   | vi          |
| LIST OF TABLES.....  | ix          |
| LIST OF FIGURES .....  | xi          |
| CHAPTER 1 INTRODUCTION .....   | 1           |
| CHAPTER 2 LITERATURE REVIEWS.....  | 3           |
| 2.1 Trace Olefins Removal from Aromatics.....                              | 3           |
| 2.2 Processing for Olefins Removal .....                                   | 4           |
| 2.2.1 Catalytic Hydrogenation.....   | 5           |
| 2.2.2 Catalytic Alkylation .....   | 6           |
| 2.3 Properties of Catalyst for Olefins Removal in Alkylation Reaction..... | 7           |
| 2.4 Types of Catalyst for Olefins Removal in Alkylation Reaction.....      | 9           |
| 2.4.1 Ionic Liquid .....   | 9           |
| 2.4.2 Sulfated Zirconia .....  | 11          |
| 2.4.3 Clay .....   | 13          |
| 2.4.4 Zeolites .....   | 16          |
| 2.3.4.1 Structure of zeolites.....   | 16          |
| 2.3.4.2 Structure of commercial zeolites.....                              | 19          |
| 2.5 Modification of Solid Acid Catalysts .....                             | 21          |
| 2.5.1 Modification of Clay .....   | 21          |
| 2.5.1.1 Clay modified with zeolite .....                                   | 21          |

|  |    |
|--|----|
| 2.5.1.2 Clay modified with metal halides.....  | 22 |
| 2.5.1.3 Acid activation of clays.....  | 24 |
| 2.5.2 Modification of Zeolite by Dealumination.....  | 26 |
| CHAPTER 3 EXPERIMENTAL.....  | 29 |
| 3.1 Materials and Equipment.....   | 29 |
| 3.1.1 Chemicals.....   | 29 |
| 3.1.2 Equipment.....   | 29 |
| 3.2 Experimental Procedures.....   | 30 |
| 3.2.1 Catalyst Preparation.....  | 30 |
| 3.2.1.1 Dealumination of USY zeolite.....  | 30 |
| 3.2.1.2 Acid activation of bentonite clay.....   | 30 |
| 3.2.2 Characterization.....  | 30 |
| 3.2.2.1 X-ray diffractometer (XRD).....  | 30 |
| 3.2.2.2 X-ray fluorescence spectrometers (XRF).....  | 31 |
| 3.2.2.3 Surface area analyzer.....   | 31 |
| 3.2.2.4 Temperature-programmed desorption/reduction/oxidation<br>analyzer (TPDRO/BELCAT II)..... | 31 |
| 3.2.2.5 Simultaneous thermal analysis.....   | 31 |
| 3.2.3 Catalytic Activity.....  | 32 |
| 3.2.4 Product Analysis.....  | 32 |
| CHAPTER 4 RESULTS AND DISCUSSION.....  | 34 |
| 4.1 Zeolites.....  | 34 |
| 4.1.1 Properties of Zeolites.....  | 35 |
| 4.1.2 Catalytic Activity of Zeolites.....  | 36 |
| 4.2 USY Modified by Dealumination with Citric Acid.....  | 38 |
| 4.2.1 Characteristics of USY and Modified USY.....   | 38 |
| 4.2.2 Catalytic Activity of Modified USY.....  | 43 |
| 4.2.3 Deactivation of USY and Modified USY.....  | 45 |
| 4.3 Clays.....   | 46 |

|  |    |
|--|----|
| 4.3.1 Properties of Clays .....  | 46 |
| 4.3.2 Catalytic Activity of Clays .....                                | 48 |
| 4.4 Bentonite Modified by Acid Activation with Hydrochloric Acid ..... | 50 |
| 4.4.1 Characteristics of Bentonite and Modified Bentonite .....        | 50 |
| 4.4.2 Catalytic Activity of Modified Bentonite .....                   | 56 |
| 4.3.3 Deactivation of Bentonite and Modified Bentonite .....           | 57 |
| 4.5 Comparasion of Modified USY and Modified bentonite .....           | 58 |
| CHAPTER 5 CONCLUSION AND RECOMMENDATION .....                          | 60 |
| 5.1 Conclusion .....   | 60 |
| 5.2 Recommendation .....   | 60 |
| APPENDICES .....   | 61 |
| Appendix A Additionnal Information .....                               | 61 |
| Appendix B Relative crystallinity (%) calculation .....                | 69 |
| REFERENCES .....   | 70 |
| VITA .....   | 73 |

## LIST OF TABLES

|   | Page |
|---|------|
| <b>Table 2.1</b> Pore diameters of ZSM-5, beta, USY, MCM-22, and sulfated zirconia.....   | 8    |
| <b>Table 2.2</b> Effect of molar fraction of zinc chloride in 1-(3-sulfopropyl)-3-methylimidazolium bromochlorozincinate on olefins conversion for alkylation reaction..... | 10   |
| <b>Table 2.3</b> Acidity of sulfated zirconia, USY, and clay .....  | 13   |
| <b>Table 2.4</b> Components of clay.....  | 13   |
| <b>Table 2.5</b> Examples of framework of zeolites.....   | 17   |
| <b>Table 2.6</b> FAU structure.....   | 19   |
| <b>Table 2.7</b> BEA structure.....   | 20   |
| <b>Table 2.8</b> MCM-22 structure.....  | 20   |
| <b>Table 2.9</b> Acidity of catalyst .....  | 22   |
| <b>Table 2.10</b> Acidity of catalyst .....   | 24   |
| <b>Table 2.11</b> Acidity of clays .....  | 25   |
| <b>Table 2.12</b> MAT result of USY and USY modified with citric acid .....   | 28   |
| <b>Table 4.1</b> Silica to alumina ratio ( $\text{SiO}_2/\text{Al}_2\text{O}_3$ ) of MCM-22, beta, USY, and mordenite .....   | 35   |
| <b>Table 4.2</b> Textural properties of MCM-22, beta, USY, and mordenite .....  | 36   |
| <b>Table 4.3</b> Acidity of MCM-22, beta, USY, and mordenite.....   | 36   |
| <b>Table 4.4</b> Initial and final olefins removal by MCM-22, beta, USY, and mordenite .  | 38   |
| <b>Table 4.5</b> Chemical compositions and crystallinity of USY and USY modified with citric acid.....  | 39   |
| <b>Table 4.6</b> Surface area and pore distribution of USY and USY modified with citric acid.....   | 42   |
| <b>Table 4.7</b> Acidity of USY and USY modified with citric acid .....   | 43   |

|   |    |
|---|----|
| <b>Table 4.8</b> Initial and final olefins removal by USY and USY modified with citric acid .....   | 45 |
| <b>Table 4.9</b> Chemical compositions of illite, bentonite, and bleaching earth .....  | 47 |
| <b>Table 4.10</b> Textural properties of clays.....   | 48 |
| <b>Table 4.11</b> Acidity of illite, bentonite, and bleaching earth.....  | 48 |
| <b>Table 4.12</b> Initial and final olefins removal by illite, bentonite, and bleaching earth.....  | 50 |
| <b>Table 4.13</b> Chemical composition of bentonite and bentonite modified with hydrochloric acid .....   | 51 |
| <b>Table 4.14</b> Surface area and pore distribution of bentonite and bentonite modified with hydrochloric acid .....                           | 54 |
| <b>Table 4.15</b> Acidity of bentonite and bentonite modified with hydrochloric acid .....  | 56 |
| <b>Table 4.16</b> Initial and final olefins removal by bentonite and bentonite modified with hydrochloric acid .....                            | 57 |
| <b>Table 4.17</b> Properties and olefins removal of modified USY and modified bentonite .....   | 59 |
| <b>Table B1</b> Intensity of the characteristic peaks at $2\theta$ of 11.9, 15.7, 18.7, 20.4, 23.7, 27.1 and 31.4 of USY and modified USY ..... | 69 |

## LIST OF FIGURES

|   | Page |
|---|------|
| <b>Figure 2.1</b> Structure of olefins. ....  | 4    |
| <b>Figure 2.2</b> Structure of aromatics. ....  | 4    |
| <b>Figure 2.3</b> Mechanism of hydrogenation reaction. ....   | 5    |
| <b>Figure 2.4</b> Reaction mechanism between 1-octene and aromatics. ....   | 6    |
| <b>Figure 2.5</b> Catalytic performance for alkylation reaction of different catalysts with different pore sizes. ....                              | 7    |
| <b>Figure 2.6</b> Olefins conversion of 1-(3-sulfopropyl)-3-methylimidazolium bromochlorozincinate on olefins removal for alkylation reaction. .... | 10   |
| <b>Figure 2.7</b> Structure of sulfated zirconia. ....  | 11   |
| <b>Figure 2.8</b> Regenerability of sulfated zirconia for removal of olefins. ....  | 12   |
| <b>Figure 2.9</b> Performance of sulfated zirconia for removal of olefins. ....   | 12   |
| <b>Figure 2.10</b> Structure of kaolinite group. ....   | 14   |
| <b>Figure 2.11</b> Structure of illite group. ....  | 15   |
| <b>Figure 2.12</b> Structure of montmorillonite/smectite group. ....  | 15   |
| <b>Figure 2.13</b> Structure of chlorite group. ....  | 15   |
| <b>Figure 2.14</b> Two-dimensional representation of the framework structure of zeolites<br>.....   | 16   |
| <b>Figure 2.15</b> Three common ways of representing a CBU. ....  | 17   |
| <b>Figure 2.16</b> Examples of some polyhedral CBUs found in known zeolite framework types. ....  | 18   |
| <b>Figure 2.17</b> Examples of chains forming. ....   | 18   |
| <b>Figure 2.18</b> Framework structure for FAU zeolite. ....  | 19   |
| <b>Figure 2.19</b> Framework structure for BEA zeolite. ....  | 20   |
| <b>Figure 2.20</b> Framework structure for MWW zeolite. ....  | 21   |

|  |    |
|--|----|
| <b>Figure 2.21</b> Bromine index of aromatics after reaction. ....   | 22 |
| <b>Figure 2.22</b> Effect of commercial clay modified with different amounts of metal halides. ....  | 23 |
| <b>Figure 2.23</b> Bromine index of olefins removal from aromatics. ....   | 23 |
| <b>Figure 2.24</b> Adsorption isotherms of nitrogen of the bentonite and modified bentonite . ....   | 25 |
| <b>Figure 2.25</b> Variation of BET surface area and pore diameter with change in acid concentrations. ....  | 26 |
| <b>Figure 2.26</b> Process of dealumination. ....  | 26 |
| <b>Figure 2.27</b> Isotherms of the USY and modified USY zeolite. ....   | 27 |
| <b>Figure 2.28</b> Profile of the mesopore distribution of USY zeolite. ....   | 27 |
| <b>Figure 3.1</b> Parr reactor. ....   | 32 |
| <b>Figure 3.2</b> Bromine index analyzer. ....   | 33 |
| <b>Figure 4.1</b> Olefins removal from aromatics in alkylation reaction by MCM-22, beta, USY, and mordenite at 195 °C and 12 barg for 6 h. ....      | 37 |
| <b>Figure 4.2</b> XRD patterns of USY and USY modified with 0.075, 0.15, and 0.3 M citric acid. ....   | 40 |
| <b>Figure 4.3</b> Isotherms of nitrogen adsorption of USY and USY modified with 0.075, 0.15, and 0.3 M citric acid. ....                             | 41 |
| <b>Figure 4.4</b> Pore size distribution of USY and USY modified with 0.075, 0.15, and 0.3 M citric acid. ....                                       | 41 |
| <b>Figure 4.5</b> NH <sub>3</sub> -TPD analysis of USY and USY modified with 0.075, 0.15, and 0.3 M citric acid. ....                                | 43 |
| <b>Figure 4.6</b> Olefins removal from aromatics in alkylation reaction by USY and USY modified with citric acid at 195 °C and 12 barg for 6 h. .... | 44 |
| <b>Figure 4.7</b> Mass change of spent USY and USY modified with 0.15 M citric acid. ....  | 46 |

|   |    |
|---|----|
| <b>Figure 4.8</b> Olefins removal from aromatics in alkylation reaction by illite, bentonite, and bleaching earth at 195 °C and 12 barg for 6 h. ....                   | 49 |
| <b>Figure 4.9</b> Relative contents of metal oxides (M/M <sub>0</sub> ) of bentonite and bentonite modified with hydrochloric acid. ....                                | 51 |
| <b>Figure 4.10</b> XRD patterns of bentonite and bentonite modified with 1, 3, and 6 M hydrochloric acid. ....  | 52 |
| <b>Figure 4.11</b> Isotherms of nitrogen adsorption of bentonite and bentonite modified with 1, 3, and 6 M hydrochloric acid. ....                                      | 53 |
| <b>Figure 4.12</b> Pore size distribution of bentonite and bentonite modified with 1, 3, and 6 M hydrochloric acid. ....  | 54 |
| <b>Figure 4.13</b> NH <sub>3</sub> -TPD analysis of bentonite and bentonite modified with 1, 3, and 6 M hydrochloric acid. ....   | 55 |
| <b>Figure 4.14</b> Olefins removal from aromatics in alkylation reaction by bentonite and bentonite modified with hydrochloric acid at 195 °C and 12 barg for 6 h. .... | 57 |
| <b>Figure 4.15</b> Mass change of spent bentonite and bentonite modified with 1 M hydrochloric acid. ....   | 58 |
| <b>Figure A1</b> X-ray diffraction (XRD) of MCM-22. ....  | 61 |
| <b>Figure A2</b> X-ray diffraction (XRD) of beta. ....  | 61 |
| <b>Figure A3</b> X-ray diffraction (XRD) of mordenite. ....   | 62 |
| <b>Figure A4</b> X-ray diffraction (XRD) of illite. ....  | 62 |
| <b>Figure A5</b> X-ray diffraction (XRD) of bleaching earth. ....   | 63 |
| <b>Figure A6</b> NH <sub>3</sub> -TPD of MCM-22. ....   | 63 |
| <b>Figure A7</b> NH <sub>3</sub> -TPD of beta. ....   | 64 |
| <b>Figure A8</b> NH <sub>3</sub> -TPD of mordenite. ....  | 64 |
| <b>Figure A9</b> NH <sub>3</sub> -TPD of illite. ....   | 65 |
| <b>Figure A10</b> NH <sub>3</sub> -TPD of bleaching earth. ....   | 65 |
| <b>Figure A11</b> Pore size distribution of MCM-22. ....  | 66 |



|   |    |
|---|----|
| <b>Figure A12</b> Pore size distribution of beta. ....            | 66 |
| <b>Figure A13</b> Pore size distribution of mordenite. ....       | 67 |
| <b>Figure A14</b> Pore size distribution of illite. ....          | 67 |
| <b>Figure A15</b> Pore size distribution of bleaching earth. .... | 68 |



3872731635

CU Theses 6171022063 thesis / recv: 20072563 15:54:37 / seq: 19

## CHAPTER 1

### INTRODUCTION

Aromatic hydrocarbons, benzene, toluene, and xylene (BTX), are important raw materials and products in the refinery and petrochemical industry. They can be obtained from cracking and/or reforming processes. However, most aromatic hydrocarbon streams from industries always contain impurities, i.e. mono-olefins, diene, styrene etc. Pu *et al.* (2012) reported that olefins can cause negative effects on following processes. In order to prevent that, the product streams need to have a bromine index (BI) lower than 20 mg/100g. Normally, hydrogenation and alkylation can be used to remove olefins. However, hydrogenation involves the use of hydrogen, resulting in the loss of aromatic products and high operating cost. Therefore, alkylation is used in most commercial processes. In the alkylation, olefins react with aromatics by using acid catalysts such as clays and zeolites to form alkyl aromatics with no further loss of aromatics.

Clays, like bentonite and illite, are used in alkylation reaction to remove trace olefins from aromatics. Clays are large pore size materials, which have cation impurities in the interlayer leading to low acid sites, which affect catalytic activity and its lifetime. Normally, the lifetime of clay is approximately 2-3 months, which is short resulting in a high operating cost. In addition, pollution and non-reusable issues are also drawbacks of using clays. In order to alleviate the challenges of using clays, acid activation of clays by mineral acids has been considered. In the acid activation, acids are used to attack in the clay structure leading to partial dissolution of the clay minerals resulting in the increase in the surface area and acidity of the material (Komadel, 2016). Sidorenko *et al.* (2018) treated illite for isomerization of  $\alpha$ -pinene oxide with hydrochloric acid and claimed that the treated illite had lower impurity and increased acidity, which enhanced the catalytic activity for isomerization. Bendou and Amrani (2014) reported that calcium in the bentonite reacted with sulfuric acid during the acid activation to form calcium sulfate leading to pore blockage. Rabie *et al.* (2018) treated bentonite for catalytic cracking process of biofuel production with hydrochloric acid. They reported that the treated bentonite had higher cracking activity due to the increased in the total acidity in bentonite.

MCM-22, USY, and beta zeolites are acid catalysts, which are more efficient than clays because zeolites can be regenerated. Chen *et al.* (2009) compared MCM-22, USY, beta, and ZSM-5 zeolites for alkylation reaction. They reported that the activity of all zeolites was similar but MCM-22 had the highest lifetime because it had large pore size. However, the price of USY is the lowest compared with MCM-22 and beta zeolites. In order to improve USY, dealumination has been used to increase the activity of catalyst.

Dealumination can be accomplished with organic or mineral acids to leach alumina from the structure of zeolites resulting in the change in the silica to alumina ratio, surface area, and acidity. However, the drawbacks of this method are the loss of crystallinity. Li *et al.* (2017) reported that the structure of modified beta zeolite with mineral acids was destroyed at a higher extent than using organic acids in the treatment. Yan *et al.* (2003) modified USY with 0.5 M citric acid for the catalytic cracking to produce LPG and diesel. They reported that the modified USY enhanced the strong acid and mesoporous property leading to the increase the catalytic activity of cracking process.

In this work, bentonite and USY zeolite were used in the alkylation reaction. The catalytic activity was investigated. In order to enhance the performance of these catalysts, bentonite was modified by acid activation by hydrochloric acid at 1 M, 3 M, and 6 M to increase acidity. USY zeolite was modified by dealumination with citric acid at 0.075 M, 0.15 M, and 0.3 M to increase surface area and proportion of strong acid to total acid sites.

## CHAPTER 2

### LITERATURE REVIEWS

#### 2.1 Trace Olefins Removal from Aromatics

Olefins, as shown in Figure 2.1, are a group of compounds made up of hydrogen and carbon that contains one or more pairs of carbon atoms linked by a double bond. Olefins are examples of unsaturated hydrocarbons (compounds that contain only hydrogen and carbon and at least one double bond). They are classified into: (1) as cyclic or acyclic (aliphatic) olefins, in which the double bond is located between carbon atoms forming part of a cyclic (closed-ring) or of an open-chain grouping, and (2) as mono-olefins, di-olefins, tri-olefins, etc., in which the number of double bonds per molecule is one, two, three, respectively. Olefins are produced via fluid catalytic cracking, hydrocracking and reforming (Sadeghbeigi, 2012).

Aromatic hydrocarbons, as shown in Figure 2.2, are a hydrocarbon with  $\sigma$  bonds and  $\pi$  electrons between carbon atoms forming a circle. The configuration of six carbon atoms in aromatic compounds is known as a benzene ring, after the simplest possible such hydrocarbon, benzene (Sadeghbeigi, 2012).

However, trace olefins are harmful to the following processes for aromatic production. In order to protect the adsorbents, which are very expensive and sensitive to olefins, the product stream must have a bromine index, which is an indicator of the presence of olefinic bonds, less than 20. Therefore, impurities must be removed with suitable treatment technologies (Pu *et al.*, 2013).

The bromine index (BI) is the number of milligram bromine ( $\text{Br}_2$ ) bound by 100 grams of sample. Normally, this method is relevant to olefin-free hydrocarbons with a bromine index lower than 1,000. Products with a bromine index greater than 1,000 are usually determined through potentiometric titration as the bromine number. To determine bromine, the element is directly generated by colometric titration. This current then releases the stoichiometrically corresponding amount of bromine from the bromide-containing reagent through electrolysis (Taylocra *et al.*, 1991).

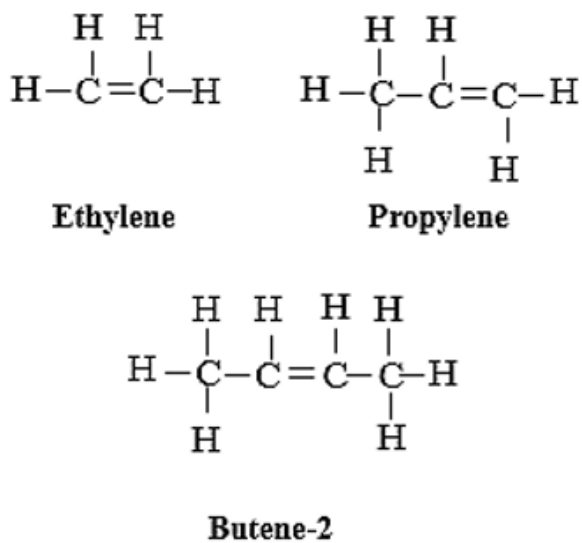


**Figure 2.1** Structure of olefins (Sadeghbeigi, 2012).

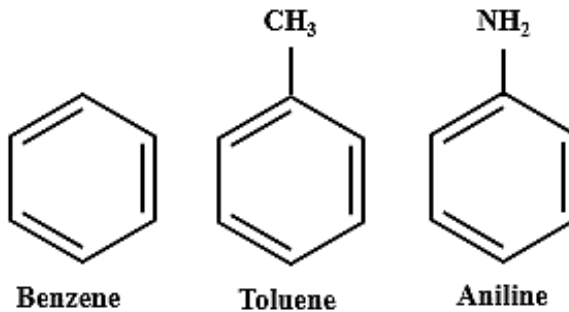


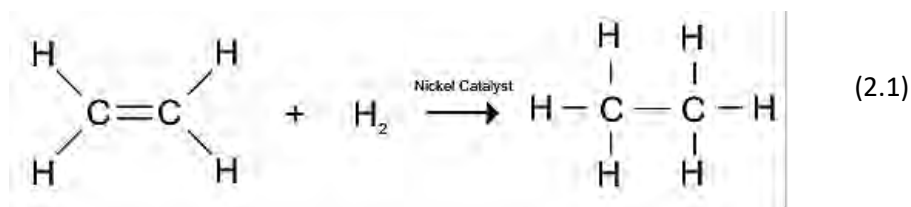
**Figure 2.2** Structure of aromatics (Sadeghbeigi, 2012).

## 2.2 Processing for Olefins Removal

There are two processes for trace olefins removal from aromatic hydrocarbons which are catalytic hydrogenation and catalytic alkylation (Li *et al.*, 2011).

### 2.2.1 Catalytic Hydrogenation

Hydrogenation plays a key role in chemical synthesis for olefins removal from aromatic hydrocarbons. Hydrogenation is a chemical reaction between molecular hydrogen and another compound or element, usually in the presence of a catalyst such as nickel, palladium or platinum as an active catalyst. This process is commonly employed to reduce or saturate organic compounds. The reaction is shown in Equation 2.1 (Pettinari *et al.*, 2004).



The mechanism of hydrogenation of alkene with nickel as a catalyst at 150°C can be described in three different steps, as shown in Figure 2.3. Firstly, hydrogen molecules react with the metal atoms at the catalyst surface. Secondly, the  $\pi$  bond of the alkene interacts with the metal catalyst weakening the bond. Lastly, the  $\pi$  bond of the alkene interacts with the metal catalyst weakening the bond (Penttinari *et al.*, 2004).

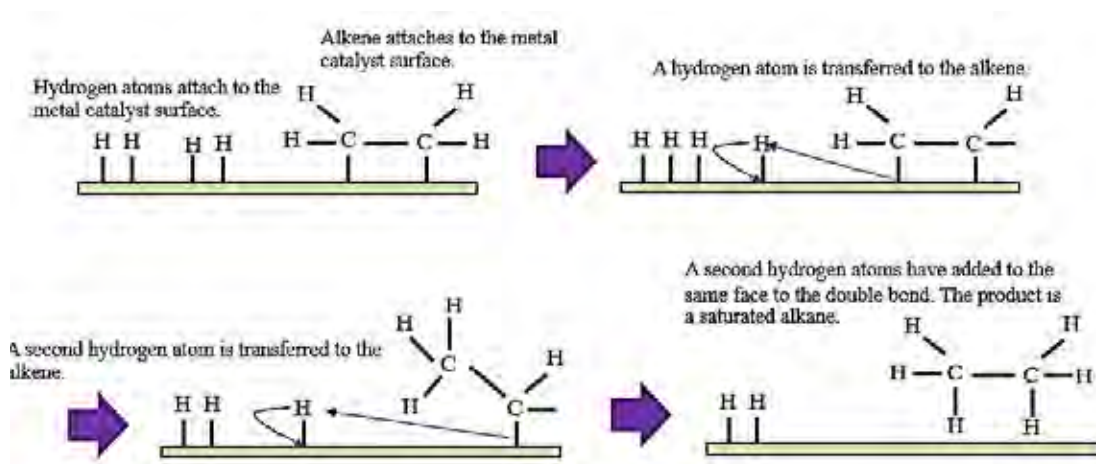


**Figure 2.3** Mechanism of hydrogenation reaction (Penttinari *et al.*, 2004).



In consideration of catalytic hydrogenation, hydrogen is used as a raw material in this reaction resulting in loss of aromatic products because of reactivity between aromatics and hydrogen. Therefore, alkylation is used commercially. Properties of catalyst for olefins removal in alkylation reaction will be discussed in section 2.3.

### 2.3 Properties of Catalyst for Olefins Removal in Alkylation Reaction

The properties of catalyst for alkylation reaction are pore diameter and acidity of catalyst. For the pore diameter of catalyst, Figure 2.5 shows that the mesoporous materials have the longest lifetime of catalyst due to they largest pore diameter (3-5 nm). On the other hand, ZSM-5 has the smallest pore diameter (0.5-0.6 nm). Therefore, it has the shortest lifetime. Table 2.1 gives the pore diameters of several catalysts (Chen *et al.*, 2009).

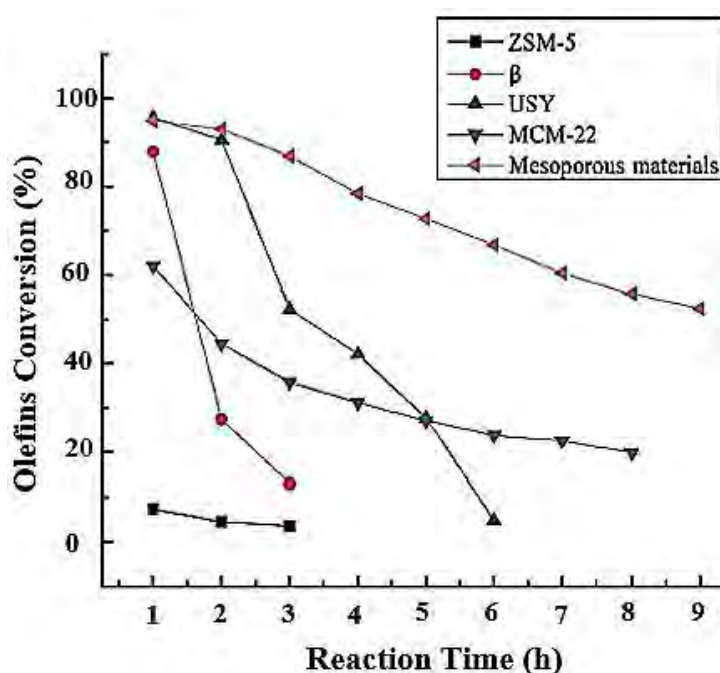


**Figure 2.5** Catalytic performance for alkylation reaction of different catalysts with different pore sizes (Chen *et al.*, 2009).



**Table 2.1** Pore diameters of ZSM-5, beta, USY, MCM-22, and sulfated zirconia (Chen *et al.*, 2009)

| Catalysts         | Pore diameter (nm) |
|-------------------|--------------------|
| ZSM-5             | 0.5-0.6            |
| Beta              | 0.75               |
| USY               | 0.9                |
| MCM-22            | 1.5                |
| Sulfated zirconia | 3-5                |

For acidity of catalyst, there are many kinds of definitions for acid. Among them, the definitions by Brønsted Lowley and Lewis are widely accepted in relation to the solid acid catalysts (Ouellette and Rawn, 2014).

Brønsted acid is a proton donor, and a Brønsted base is a proton acceptor. When a surface site has a property of proton donation, the site is called Brønsted acid sites. Equation 2.3 shows the definition of Brønsted Lowley.



Lewis acid is a chemical species being able to accept electron-pair (electron acceptor). When a surface site has the property of electron pair acceptor, the site is called Lewis acid site. Equation 2.4 shows definition of Lewis acid.



In order to increase catalytic activity and lifetime of catalyst for alkylation reaction, Brønsted and Lewis acids of a catalyst must be optimized. If the catalyst has high Brønsted acid site, the olefins removal is high causing the catalyst deactivation (Pu *et al.*, 2013). Therefore, sections 2.4 and 2.5 will discuss about types of catalyst and modification of catalysts for olefins removal in alkylation reaction.

## 2.4 Types of Catalyst for Olefins Removal in Alkylation Reaction

There are many types of acid catalyst which are used in catalytic alkylation, i.e., ionic liquids, sulfated zirconia, clays, and zeolites. The definition for acid catalyst will be discussed in this section.

### 2.4.1 Ionic Liquid

An ionic liquid is a salt in the liquid state, which results in these solvents being liquid below 100 °C or even at room temperature. At least one ion has a delocalized charge and one component is organic, which prevents the formation of a stable crystal lattice. Examples of ionic liquid are 1-(3-sulfopropyl)-3-methylimidazolium ( $C_3SO_3Hmim$ ), n-butylpyridinium bromide ([BuPy]Br) and 1-butyl-3-methylimidazolium bromide ([BMIm]Br). Tian *et al.* (2013) used 1-(3-sulfopropyl)-3-methylimidazolium doped with bromochlorozincinate to increase the acidity for olefins removal from aromatics in alkylation reaction. The olefins conversion increased significantly when the molar fraction of zinc chloride increased from 0 to 0.67, as shown in Table 2.2. That is because of the increase in the acidity. Figure 2.6 presents the olefins conversion of 1-(3-sulfopropyl)-3-methylimidazolium bromochlorozincinate with 0.67 molar fraction of zinc chloride at 100 °C and atmospheric pressure. The olefins conversion was 30% at the reaction time of 3 h.

The olefins conversion of ionic liquids is low compared with other acid catalysts. Moreover, ionic liquids are a homogenous catalyst, which is difficult to remove from the process. Therefore, ionic liquids may not be suitable for using in a commercial scale.

**Table 2.2** Effect of molar fraction of zinc chloride in 1-(3-sulfopropyl)-3-methylimidazolium bromochlorozincinate on olefins conversion for alkylation reaction (Tian *et al.* 2013)

| Mole fraction of zinc chloride | Olefins conversion (%) |
|--------------------------------|------------------------|
| 0                              | 2.97                   |
| 0.5                            | 4.36                   |
| 0.6                            | 7.05                   |
| 0.67                           | 16.29                  |
| 0.71                           | 17.94                  |
| 0.75                           | 11.03                  |

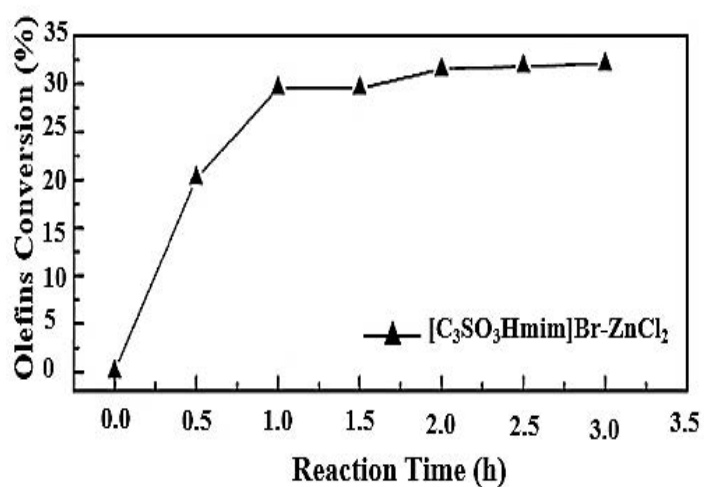


**Figure 2.6** Olefins conversion of 1-(3-sulfopropyl)-3-methylimidazolium bromochlorozincinate on olefins removal for alkylation reaction (Tian *et al.* 2013).

### 2.4.2 Sulfated Zirconia

Sulfated zirconia (SZ) is a superacid catalyst. It has a mesoporous material, which is used in many reactions, i.e. isomerization, acylation, esterification, and alkylation reaction of olefins removal from aromatics. Sulfated zirconia is zirconium oxide or zirconia modified with sulfate ions. The structure of sulfated zirconia is illustrated in Figure 2.7.

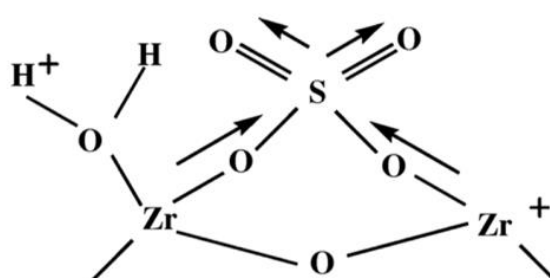


**Figure 2.7** Structure of sulfated zirconia (Hino *et al.*, 2006).

Yao *et al.* (2015) studied sulfated zirconia as a novel catalyst for trace olefins removal from aromatics. Important factors for catalytic activity of sulfated zirconia are high weak Lewis acid and mesoporous size (>2nm). Moreover, sulfated zirconia is an acid catalyst, which can be regenerated. Figure 2.8 presents regenerability of sulfated zirconia. The removal of olefins remains over 90% during the first 6 h of reaction time using the recovered sulfated zirconia for the third time. Figure 2.9 compares the performance of sulfated zirconia (black line), USY (red line), and active clay (blue line). The results show that initial conversion of USY is the highest due to the highest acidity, which is shown in Table 2.3, but the stability of sulfated zirconia is the best because of its high weak Lewis acid.

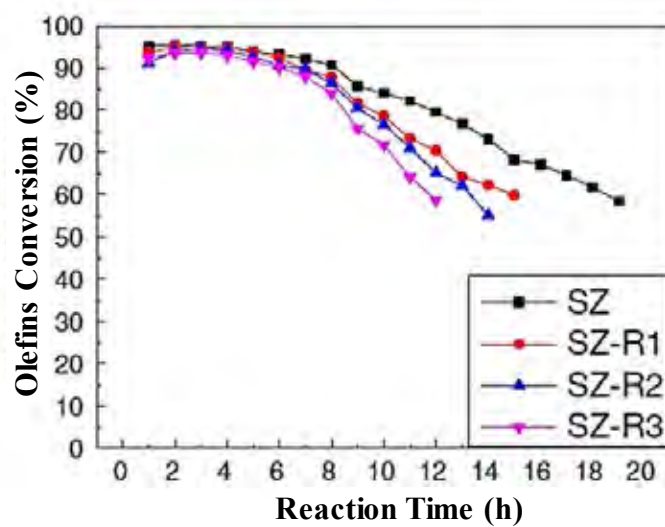


**Figure 2.8** Regenerability of sulfated zirconia for removal of olefins (Yao *et al.*, 2015).

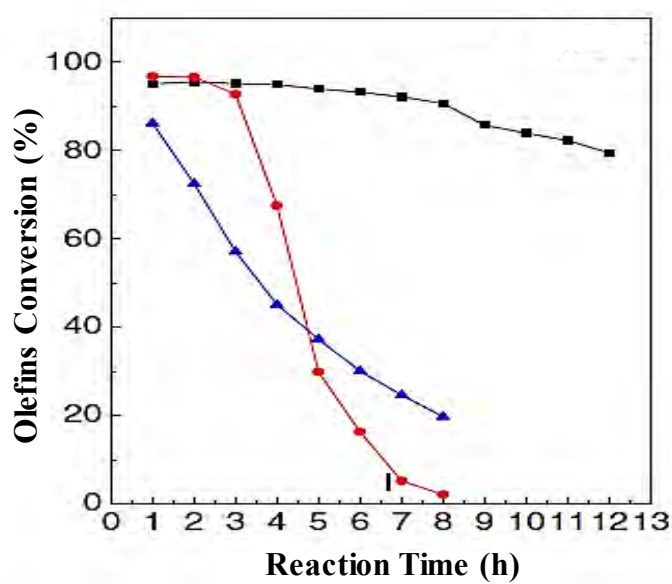


**Figure 2.9** Performance of sulfated zirconia for removal of olefins (Yao *et al.*, 2015).



3872731635

**Table 2.3** Acidity of sulfated zirconia, USY, and clay (Yao *et al.*, 2015)

| Sample | Acidity ( $\times 10^{-4}$ mol/g) |                  |                     |
|--------|-----------------------------------|------------------|---------------------|
|        | Total acid                        | Weak Lewis sites | Total Brønsted acid |
| SZ     | 92.7                              | 39.1             | 35.6                |
| USY    | 784.4                             | 6.7              | 777.3               |
| Clay   | 31.8                              | 8.6              | 19.5                |

However, cost of sulfated zirconia is expensive compared with zeolites and clays. Moreover, it has sulfur leaching in the process leading to environmental problems. Therefore, sulfated zirconia is still not suitable for commercial scale.

#### 2.4.3 Clay

Clay minerals are a group of hydrous aluminosilicates, sometimes with variable amounts of iron, magnesium, alkali metals, alkaline earths, and other cations. The composition of clay is shown in Table 2.4. These minerals are similar in chemical and structural composition to the primary minerals originated from the Earth's crust. Clay can be divided into mainly 4 types: kaolinite group, montmorillonite/smectite group, illite group, and chlorite group (Murray, 2006).

**Table 2.4** Components of clay (Pu *et al.*, 2012)

| Components                     | Content (wt%) |
|--------------------------------|---------------|
| SiO <sub>2</sub>               | 60.3          |
| Al <sub>2</sub> O <sub>3</sub> | 15.3          |
| Fe <sub>2</sub> O <sub>3</sub> | 7.8           |
| CaO                            | 2.1           |
| MgO                            | 7.3           |
| K <sub>2</sub> O               | 1.6           |
| Na <sub>2</sub> O              | 0.9           |
| Others                         | 4.7           |

The kaolinite group, which is shown in Figure 2.10, composes of polymorphs of formula  $\text{Al}_2\text{Si}_2\text{O}_5(\text{OH})_4$ . The repeat unit is a single silicate sheet condensed with alumina octahedra and also includes dickite and nacrite, formed by the decomposition of orthoclase feldspar (e.g. in granite) (Murray, 2006).

The general formula of illite group is  $(\text{K},\text{H})\text{Al}_2(\text{Si},\text{Al})_4\text{O}_{10}(\text{OH})_{2-x}\text{H}_2\text{O}$ , where  $x$  represents a variable amount of water. The structure of this group, which is shown in Figure 2.11, is similar to the montmorillonite group with a sandwich-type structure and also includes glauconite and are the commonest clay minerals (Murray, 2006).

The montmorillonite/smectite group includes talc, vermiculite, montmorillonite, and others. The general formula is  $(\text{Ca},\text{Na},\text{H})(\text{Al},\text{Mg},\text{Fe},\text{Zn})_2(\text{Si},\text{Al})_4\text{O}_{10}(\text{OH})_{2-x}\text{H}_2\text{O}$ , where  $x$  represents a variable amount of water. These minerals all have the sandwich structure with tetrahedral silicate layers strongly bonded to octahedral aluminum or magnesium atoms i.e. bentonite and vermiculite. The structure of montmorillonite is shown in Figure 2.12 (Murray, 2006).

The chlorite group also contains sandwich-type units. In many of these minerals, there is another weakly attached, octahedrally coordinated  $\text{Mg}^{2+}$  between sandwiches. The general formula is  $\text{X}_{4-6}\text{Y}_4\text{O}_{10}(\text{OH}, \text{O})_8$ . The  $\text{X}$  represents either aluminum, iron, lithium, magnesium, manganese, nickel, zinc or rarely chromium. The  $\text{Y}$  represents either aluminum, silicon, boron or iron but mostly aluminum and silicon. The structure of chlorite is shown in Figure 2.13 (Murray, 2006).

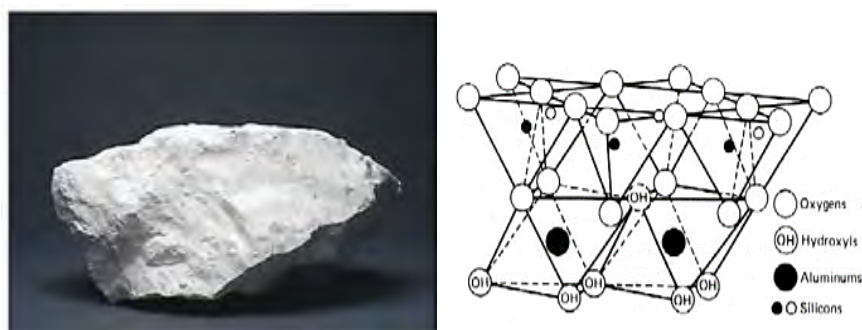


**Figure 2.10** Structure of kaolinite group (Murray, 2006).

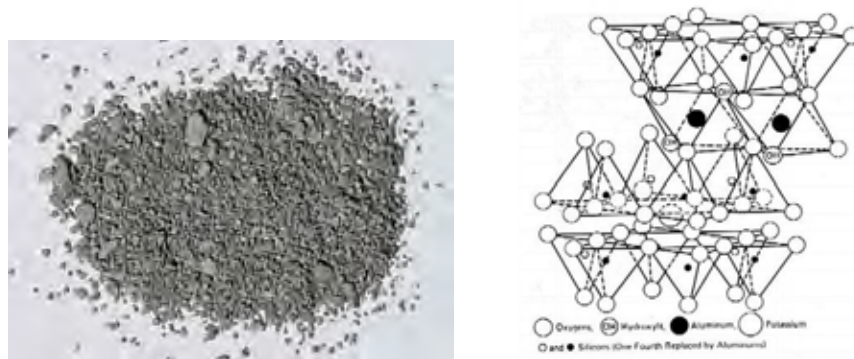


Figure 2.11 Structure of illite group (Murray, 2006).

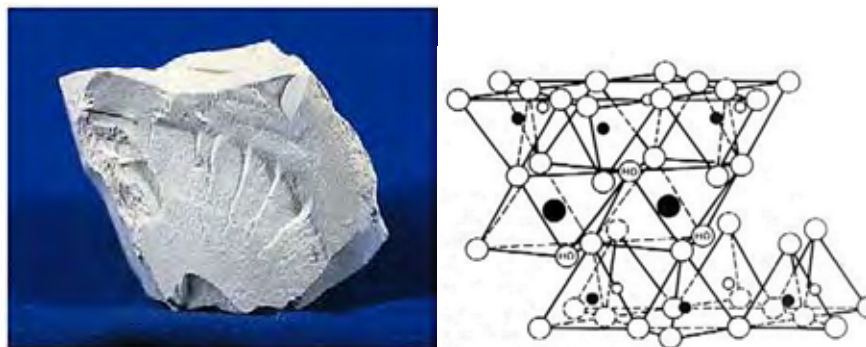


Figure 2.12 Structure of montmorillonite/smectite group (Murray, 2006).

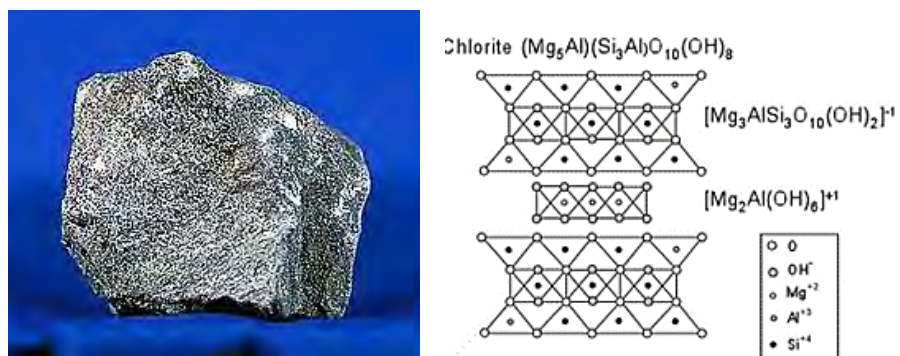


Figure 2.13 Structure of chlorite group (Haydn *et al.*, 2006).



#### 2.4.4 Zeolites

Zeolites are aluminosilicate materials, which are extensively used in commercial and environmental applications due to their unique physical and chemical properties. They are used in petrochemical industries and refineries because of the low cost of the raw materials, extremely porous structure, robust physical properties and useful chemical properties.

Zeolites are microporous crystalline aluminosilicates, composed of  $\text{TO}_4$  tetrahedra ( $T = \text{Si}, \text{Al}$ ) with O atoms connecting neighboring tetrahedra. For a completely siliceous structure, combination of  $\text{TO}_4$  ( $T = \text{Si}$ ) units in this fashion leads to silica ( $\text{SiO}_2$ ), which is an uncharged solid. Upon incorporation of Al into the silica framework, the +3 charge on the Al makes the framework negatively charged and requires the presence of extraframework cations (inorganic and organic cations can satisfy this requirement) within the structure to keep the overall framework neutral. The framework of zeolites is illustrated in Figure 2.14 (Cejka *et al.*, 2009).

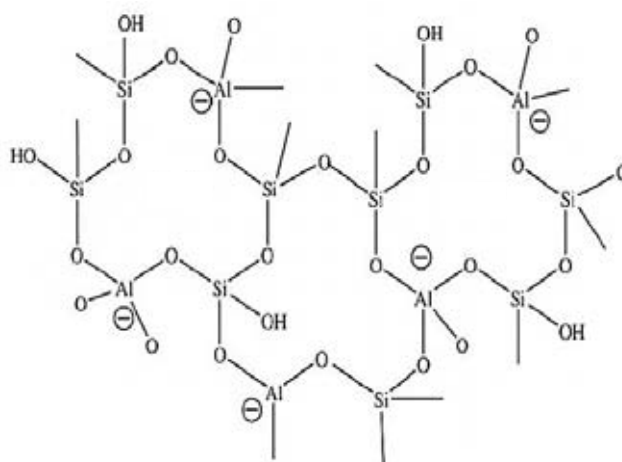


**Figure 2.14** Two-dimensional representation of the framework structure of zeolites (Auerbach *et al.*, 2003).

##### 2.3.4.1 Structure of zeolites

Zeolites can be classified by considering the topology of the framework regardless chemical composition. All zeolites having the same topology constitute a zeolite framework type. There are 191 known framework types

recognized by the Structure Commission of the International Zeolite Association (IZA) assigned with three-letter code. Table 2.5 shows examples of framework of zeolites (Baerlocher *et al.*, 2001).

**Table 2.5** Examples of framework of zeolites (Baerlocher *et al.*, 2001)

| Silicate | Phosphate |
|----------|-----------|
| MWW      | ACO       |
| MFI      | AEI       |
| BEA      | SAO       |
| FAU      | SAS       |

The basic building unit (BBU) for the framework in a zeolite is a  $TO_4$  tetrahedron, where the central T-atom is typically Si or Al and the peripheral atoms are O. It is sometimes convenient to discuss composite building units (CBUs) formed by combining several BBUs. Three common ways of representing a CBU are shown in Figure 2.15 (Flanigen *et al.*, 2010).

Polyhedral CBUs are described using common names (such as sodalite cage), three letter codes (such as d4r), or the descriptors  $[n_1^{m_1} n_2^{m_2} \dots]$ , where  $m_1$  is the number of  $n_1$ -rings,  $m_2$  is the number of  $n_2$ -rings, etc. Examples of some polyhedral CBUs found in known zeolite framework types are shown in Figure 2.16. Examples of chains forming are shown in Figure 2.17 (Flanigen *et al.*, 2010).

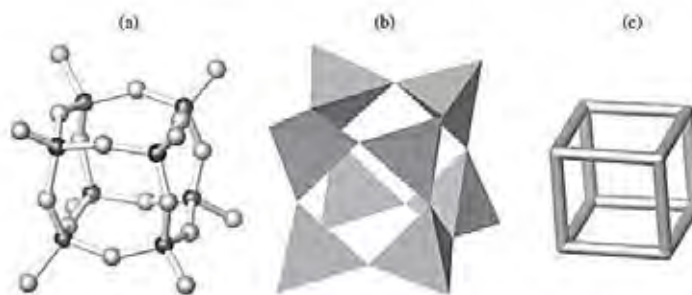


**Figure 2.15** Three common ways of representing a CBU (Flanigen *et al.*, 2010).

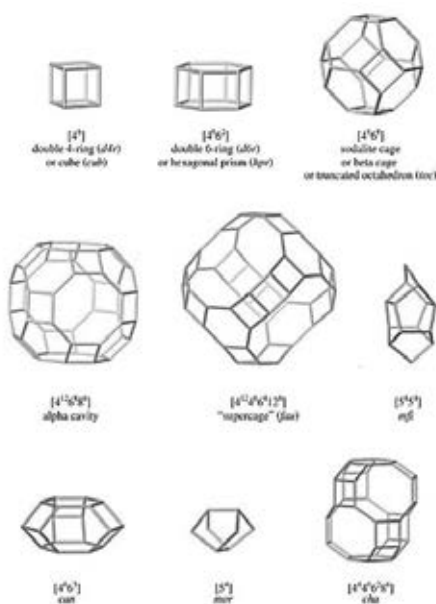


**Figure 2.16** Examples of some polyhedral CBUs found in known zeolite framework types (Flanigen *et al.*, 2010).

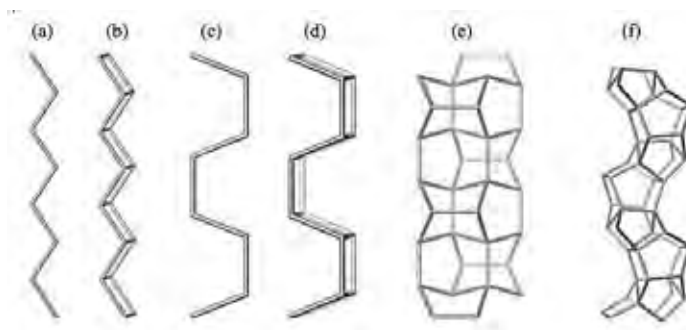


**Figure 2.17** Examples of chains forming (Flanigen *et al.*, 2010).

The  $n$ -rings (where  $n$  is the number of T atoms in the ring) defining the face of a polyhedral CBU are called pores. Polyhedral whose faces are no larger than six - rings are called cages, because the faces are too narrow to pass molecules larger than  $\text{H}_2\text{O}$ . Polyhedral with at least one face larger than a six-ring are called cavities. Pores that are infinitely extended in one dimension and are large enough to allow diffusion of guest species (i.e., larger than six-rings) are called channels. Framework types can contain one-, two-, or three-dimensional channels.

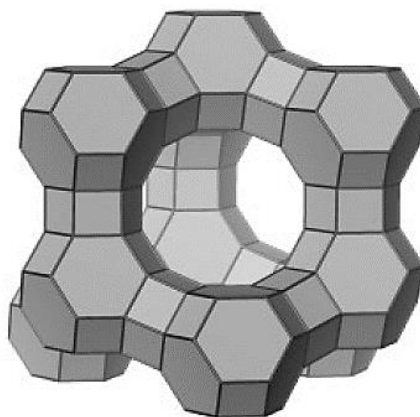
### 2.3.4.2 Structure of commercial zeolites

Commercially significant zeolites include the synthetic zeolites type A (LTA), X (FAU), Y (FAU), L (LTL), mordenite (MOR), ZSM-5(MFI), beta (\*BEA/BEC), and MCM-22 (MWW) and the natural zeolites mordenite (MOR) and chabazite (CHA).

The FAU framework type, as shown in Table 2.6, can be built by linking sodalite cages through double 6 -rings. Structure of FAU is illustrated in Figure 2.18.

**Table 2.6** FAU structure (Flanigen *et al.*, 2010)

| Type material    | Faujasite   |
|------------------|---|
| Chemical formula | $[(Ca,Mg,Na)_{29}(H_2O)_{240}][Al_{58}Si_{134}O_{384}]$ |
| Space group      | Cubic, Fd-3m, a = 34.74 Å                               |
| Pore structure   | Three-dimensional 12-ring                               |
| Mineral form     | Faujasite   |

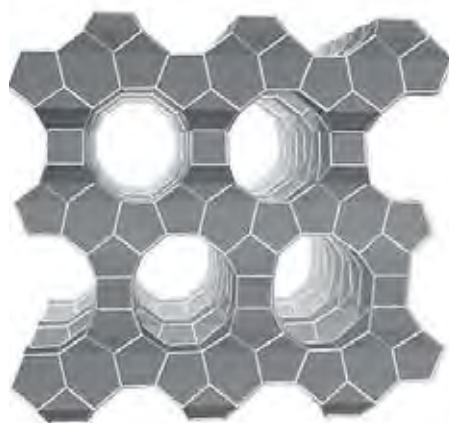


**Figure 2.18** Framework structure for FAU zeolite (Flanigen *et al.*, 2010).

The BEA framework type, as shown in Table 2.7, can be built by linking sodalite cages through 12 -rings. Structure of BEA is illustrated in Figure 2.19.

**Table 2.7** BEA structure (Flanigen *et al.*, 2010)

| Type material    | Beta  |
|------------------|---|
| Chemical formula | $[\text{Na}_7][\text{Al}_7\text{Si}_{57}\text{O}_{128}]$                      |
| Space group      | Tetragonal, $P4_122$ , $a = 12.661 \text{ \AA}$ ,<br>$c = 26.406 \text{ \AA}$ |
| Pore structure   | Three-dimensional 12-ring   |
| Mineral form     | Tschernichite   |

**Figure 2.19** Framework structure for BEA zeolite (Flanigen *et al.*, 2010).

The MCM framework type, as shown in Table 2.8, contains 2 dimensional through 10-rings and 12-rings. Structure of MWW is illustrated in Figure 2.20.

**Table 2.8** MCM-22 structure (Flanigen *et al.*, 2010)

| Type material    | MCM-22   |
|------------------|--|
| Chemical formula | $[\text{H}_{2.4}\text{Na}_{3.1}][\text{Al}_{0.4}\text{B}_{5.1}\text{Si}_{66.5}\text{O}_{144}]$ |
| Space group      | Hexagonal, $P6/mmm$ , $a = 14.208 \text{ \AA}$ ,<br>$c = 24.945 \text{ \AA}$                   |
| Pore structure   | Two-dimensional 10-ring  |
| Mineral form     | Not Known  |

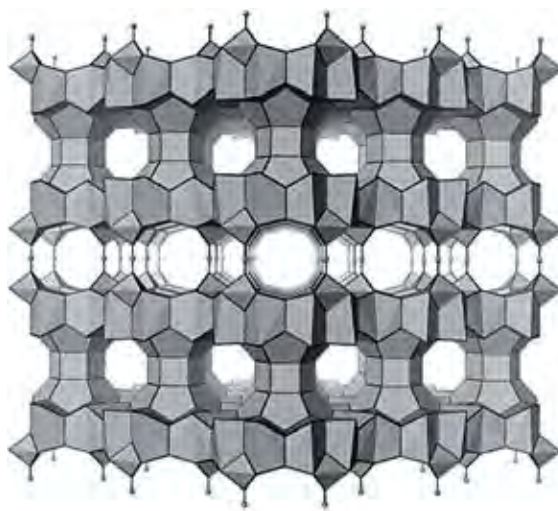


**Figure 2.20** Framework structure for MWW zeolite (Flanigen *et al.*, 2010).

## 2.5 Modification of Solid Acid Catalysts

Clays and zeolites as an popular acid catalyst, which are used to remove olefins from aromatics. In this section, clays and zeolites are modified in order to enhance pore size, mesoporous property, and acidity.

### 2.5.1 Modification of Clay

#### 2.5.1.1 *Clay modified with zeolite*

Pu *et al.* (2012) studied comercial clay modified with MCM-22 for olefins removal in alkylation reaction. The ratio of commercial clay and MCM-22 was 4. The  $\text{SiO}_2/\text{Al}_2\text{O}_3$  ratio and pore diameter of MCM-22 is 30 and 0.7 nm respectively. Figure 2.21 shows that modified catalyst can increase lifetime 5.3 times with the bromine index lower than 20 mgBr/100 g sample compared with comercial clay because modified catalyst had higher acidity, especially weak Lewis acid, which is shown in Table 2.9.

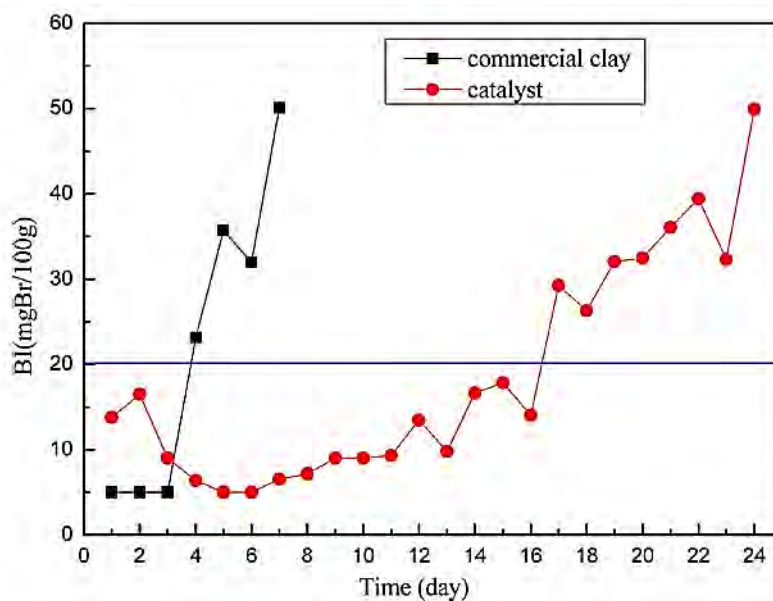


**Figure 2.21** Bromine index of aromatics after reaction (Pu *et al.*, 2012).

**Table 2.9** Acidity of catalyst (Pu *et al.*, 2012)

| Sample   | Acidity ( $\times 10^{-4}$ mol/g) |                   |                 |
|----------|-----------------------------------|-------------------|-----------------|
|          | Total Lewis acid                  | Strong Lewis acid | Weak Lewis acid |
| Catalyst | 3.17                              | 0.24              | 2.93            |
| Clay     | 0.32                              | 0.14              | 0.18            |
| MCM-22   | 25.39                             | 18.69             | 6.70            |

### 2.5.1.2 Clay modified with metal halides

Li *et al.* (2011) modified commercial clay with metal halides ( $\text{AlCl}_3$ ,  $\text{CeCl}_3$ , and  $\text{ZnCl}_2$ ) by varying metal loading (1 – 10 wt%) for olefins removal with alkylation. The result shows that the modified catalyst enhanced the acidity with the increase in the metal loading leading to the increase in the olefins conversion, as shown in Table 2.10. Figure 2.22 shows that olefins conversion of modified catalyst with 7 wt% is as same as with 10 wt%. Moreover, the modified catalyst increased its lifecycle time 5 times with the bromine index lower than 20 mgBr/100 g sample compared with commercial clay as, shown in Figure 2.23.

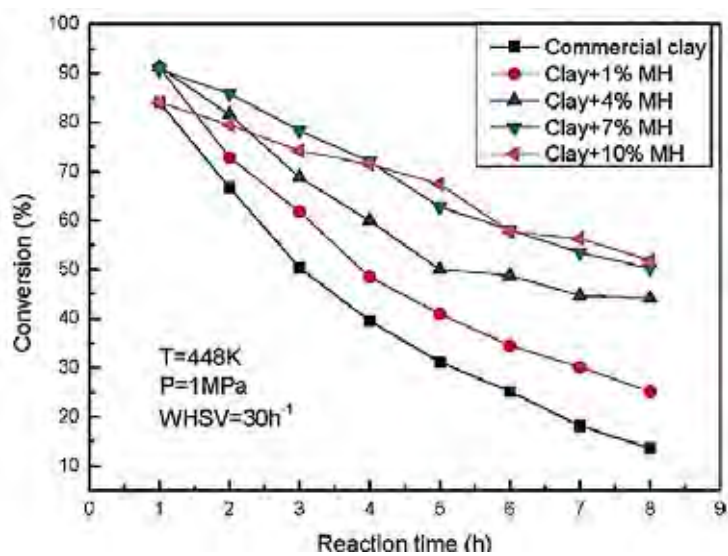


**Figure 2.22** Effect of commercial clay modified with different amounts of metal halides (Li *et al.*, 2011).

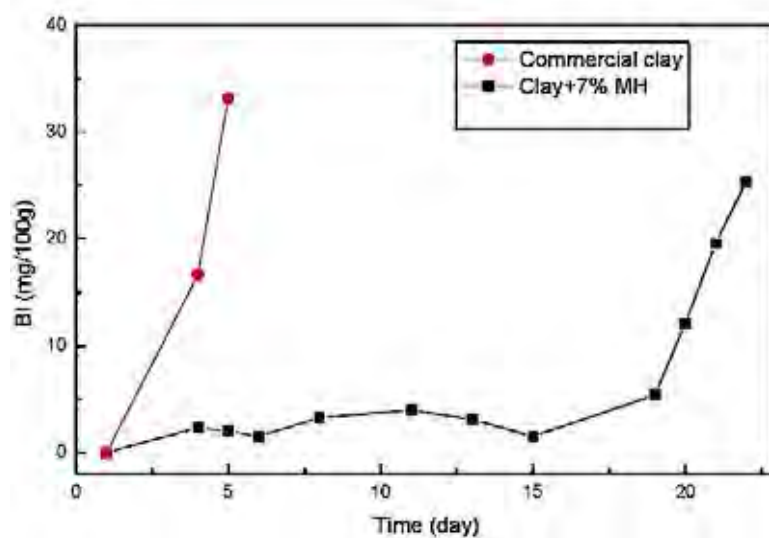


**Figure 2.23** Bromine index of olefins removal from aromatics (Li *et al.*, 2011).



**Table 2.10** Acidity of catalyst (Li *et al.*, 2011)

| Sample          | Acidity ( $\times 10^{-4}$ mol/g) |                   |                 |
|-----------------|-----------------------------------|-------------------|-----------------|
|                 | Total Lewis acid                  | Strong Lewis acid | Weak Lewis acid |
| Commercial clay | 0.34                              | 0.12              | 0.22            |
| Clay+1 wt.%MH   | 0.68                              | 0.30              | 0.38            |
| Clay+4 wt.%MH   | 1.28                              | 0.39              | 0.89            |
| Clay+7 wt.%MH   | 3.11                              | 0.15              | 2.96            |
| Clay+10 wt.%MH  | 3.42                              | 0.12              | 0.30            |

### 2.5.1.3 Acid activation of clays

Acid activation is a chemical treatment that is used on clays by using mineral acid, i.e. hydrochloric acid or sulfuric acid. Normally, clays have cations as an impurity on the interlayer. Cations will block the active sites on clays causing the low acid sites. In the acid activation, acids would attack cations leading to partial dissolution of the clay minerals resulting in the increase in the surface area and acidity (Komadel, 2016).

Sidorenko *et al.* (2018) treated illite for isomerization of  $\alpha$ -pinene oxide with hydrochloric acid by varying the acid concentration. They indicated that when the acid concentration increased, the total acidity and L/B ratio increased, as shown in Table 2.11. The source of Lewis acid of illite is aluminium ions located on the surface of their tetrahedral layer but the source of Brønsted acid of illite is the water molecules associated with aluminium ions undergone polarization on their octahedral layer. During acid activation of illite, the washing out of tetrahedral aluminium ion occurred at the slower extent than octahedral aluminium ion resulting in increasing the L/B ratio from 1.6 to 6.7 with the increase in the hydrochloric concentration from 5 wt% to 30 wt%.

Yildiz *et al.* (2004) studied the surface properties of bentonite after acid activation using different concentrations of sulfuric acid (0.5 - 4 M). Figure 2.24 shows that the adsorption isotherms of nitrogen on both bentonite and modified bentonite are similar. Figure 2.25 shows the variation of BET surface areas and mean pore diameter. The BET surface area of sample activated with 2 M was the maximum



3872731635

CD IThesis 6171022063 thesis / rev: 20072563 15:54:37 / seq: 19

(240.9 m<sup>2</sup>/g) and decreased with the increase in the acid concentration up to 4 M because higher acid concentration caused the structural change and partial decomposition of montmorillonite.

**Table 2.11** Acidity of clays (Sidorenko *et al.*, 2018)

| Aluminosilicate | Acid site concentration ( $\times 10^{-4}$ mol/g) |        |        |       |        |        | Total | L/B |
|-----------------|---|--------|--------|-------|--------|--------|-------|-----|
|                 | Brønsted  |        |        | Lewis |        |        |       |     |
|                 | Weak  | Medium | Strong | Weak  | Medium | Strong |       |     |
| 5 wt% HCl       | 0.08  | 0.06   | 0      | 0.08  | 0.14   | 0      | 0.36  | 1.6 |
| 10 wt% HCl      | 0.05  | 0.05   | 0.02   | 0.22  | 0.09   | 0.04   | 0.47  | 2.9 |
| 20 wt% HCl      | 0   | 0.01   | 0.03   | 0.11  | 0.07   | 0.04   | 0.26  | 5.5 |
| 30 wt% HCl      | 0.01  | 0.02   | 0      | 0.10  | 0.10   | 0      | 0.23  | 6.7 |

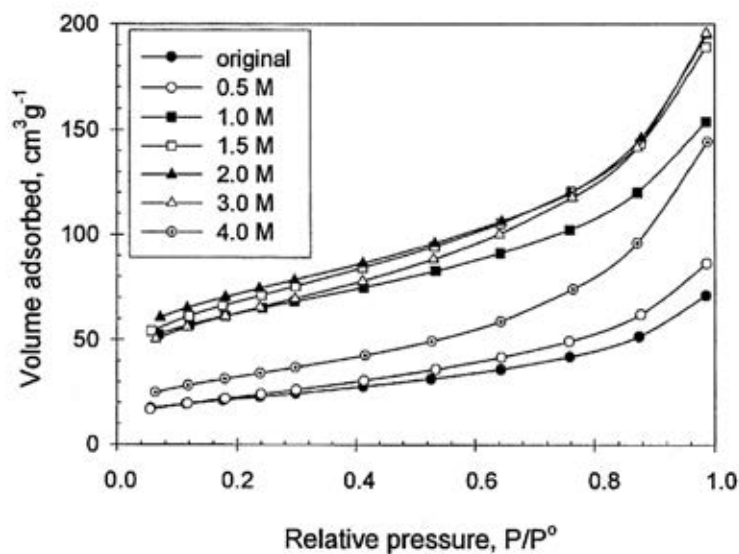


**Figure 2.24** Adsorption isotherms of nitrogen of the bentonite and modified bentonite (Yildiz *et al.* 2004).

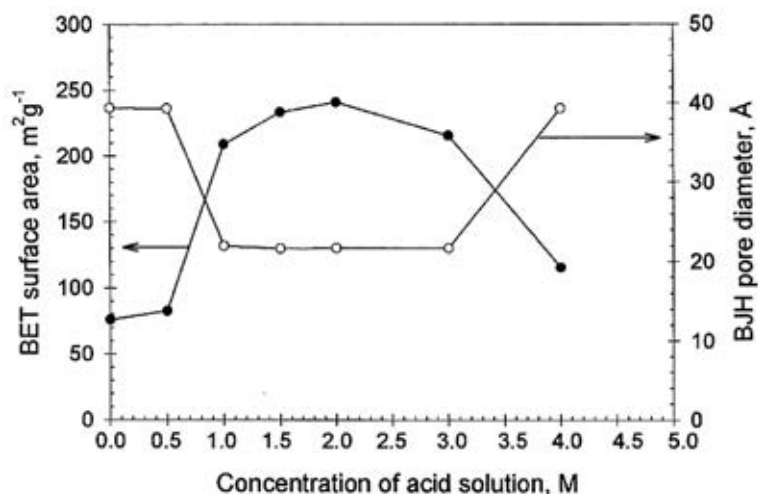


**Figure 2.25** Variation of BET surface area and pore diameter with change in acid concentrations (Yildiz *et al.*, 2004).

### 2.5.2 Modification of Zeolite by Dealumination

Dealumination is a post-synthesis method, which can be used to remove aluminium species from zeolite framework to increase secondary mesopore. There are three methods for dealumination, which are hydrothermal, acid-leaching, and chemical agent. The process of dealumination is shown in Figure 2.26 (Beyer, 2002).

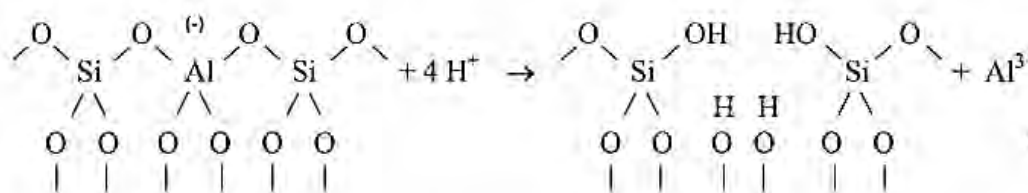


**Figure 2.26** Process of dealumination (Beyer, 2002).

Xin-Mei and Zi-Feng (2001) modified USY with 0.5 M citric acid in fluid catalytic cracking (FCC) process. Figure 2.27 shows that the adsorption isotherms of nitrogen on both USY and modified USY are type IV. The result shows that the USY modified with citric acid increased pore volume on both of micropore and mesopore, as shown in Figure 2.28. Increasing the micropore produced more

LPG and gasoline products resulting in increasing the catalytic activity. Moreover, increasing the mesopore reduced the coke formation in the fluid catalytic cracking, as shown in Table 2.13.

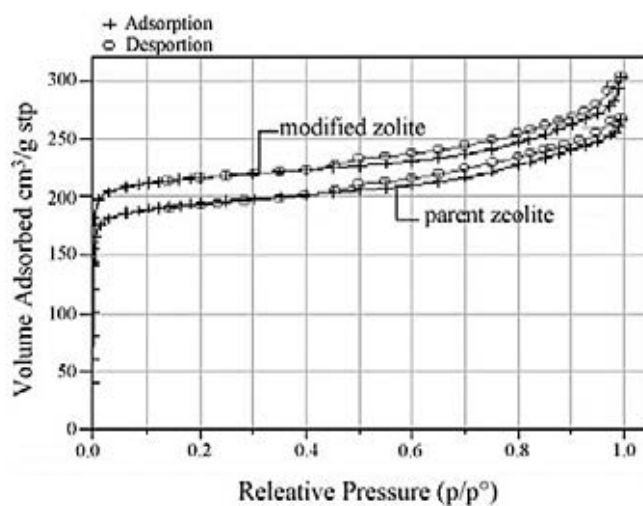


**Figure 2.27** Isotherms of the USY and modified USY zeolite (Xin-Mei and Zi-Feng, 2001).

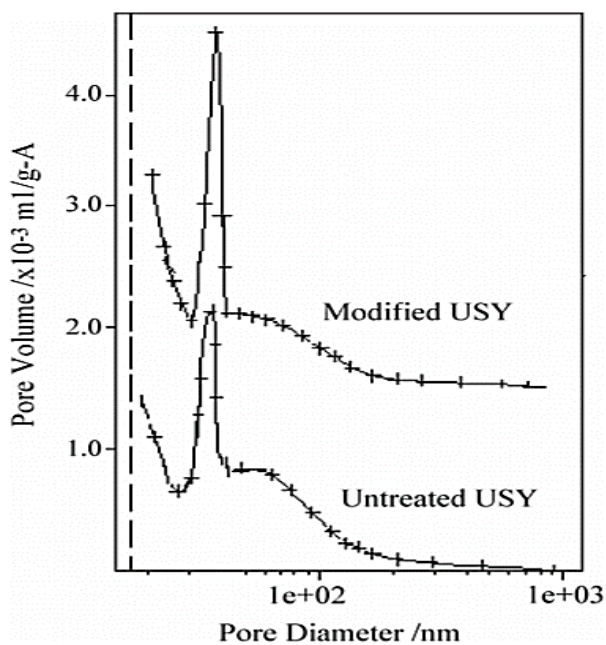


**Figure 2.28** Profile of the mesopore distribution of USY zeolite (Xin-Mei and Zi-Feng, 2001).

**Table 2.12** MAT result of USY and USY modified with citric acid (Xin-Mei and Zi-Feng, 2001)

| <b>Sample</b> | <b>Acitivity (%)</b> | <b>LPG (wt%)</b> | <b>Gasoline (wt%)</b> | <b>Diesel (wt%)</b> | <b>Coke (wt%)</b> |
|---------------|----------------------|------------------|-----------------------|---------------------|-------------------|
| USY           | 60                   | 14.39            | 35.19                 | 18.38               | 5.75              |
| USY-0.5 M     | 70                   | 17.70            | 19.30                 | 20.92               | 3.01              |



3872731635

CU IThesis 6171022063 thesis / recv: 20072563 15:54:37 / seq: 19

## CHAPTER 3

### EXPERIMENTAL

#### 3.1 Materials and Equipment

##### 3.1.1 Chemicals

1. Citric Acid monohydrous (AR grade, 99.8% purity, Loba Chemie, India)
2. USY, MCM-22, Beta, Mordenite (Nankai University, China)
3. Bentonite (Ceramic R US Co., Ltd, Thailand)
4. Illite (Thailand)
5. Bleaching earth (India)
6. Heavy reformat (Thai Oil Public Co., Ltd, Thailand)
7. Potassium bromide (AR grade, 99.5% purity, Loba Chemie, India)
8. Glacial acetic acid (AR grade, Quality Reagent Chemical, New Zealand)
9. Methanol (AR grade, Macron, US)
10. Hydrochloric acid (AR grade, 37% w/w, Merck, Germany)
11. Toluene (AR grade, 99.9% purity, Merck, Germany)
12. Deionized water

##### 3.1.2 Equipment

1. High pressure reactor (PARR reactor)
2. Bromine index analyzer (Titrand 851 Metrohm)
3. Controlable water bath
4. Hot oil bath
5. Magnatic stirrer
6. Vacuum pump
7. Oven
8. Calcination furnance
9. Surface area analyzer (Quantachrome, Autosorb 1-MP)

10. X-ray diffractometer (XRD Rigaku, Smartlab)
11. Temperature-programmed desorption /oxidation analyzer (TPDRO/BELCAT II)
12. X-ray fluorescence spectrometer (XRF BRUKER S8 TIGER)
13. Simultaneous thermal analysis (NETZSCH STA 449F3)

## 3.2 Experimental Procedures

### 3.2.1 Catalyst Preparation

#### 3.2.1.1 Dealumination of USY zeolite

The modified USY was prepared by dealumination method. 15 g of USY zeolite and 150 ml of citric acid were placed into a three-necked flask equipped with a reflux condenser. The solution was stirred for 4 h at 90 °C. Then, the sample was filtered and washed with deionized water. Finally, the sample was dried in an oven at 120 °C overnight. The series of modified USY zeolite were prepared with an acid solution (0.075, 0.15, and 0.3 M). If the sample was treated by 0.075 M citric acid, it is denoted by USY-0.075.

#### 3.2.1.2 Acid activation of bentonite clay

The modified bentonite was prepared by acid activation method. 20 g of bentonite and 100 ml of hydrochloric acid were placed into beaker. The solution was stirred for 1 h at room temperature. Then, the sample was washed and centrifuged until no chloride ion in the solution was detected. Finally, the sample was dried in an oven at 120 °C overnight. The series of modified bentonite were prepared with an acid solution (1, 3, and 6 M). If the sample was treated by 1 M hydrochloric acid, it is denoted by Ben-1.

### 3.2.2 Characterization

#### 3.2.2.1 X-ray diffractometer (XRD)

The X-Ray diffraction (XRD) patterns of samples were obtained using a Bruker X-Ray diffractometer system (D8 Advance) with a  $\text{CuK}\alpha$  radiation (1.5405 Å). XRD was operated at 40 kV and 100 mA. The measurement conditions

were in the range of  $2\theta = 5^\circ$  to  $55^\circ$  with the scan speed of  $4^\circ/\text{min}$  and the scan step of  $0.02^\circ$ .

#### 3.2.2.2 X-ray fluorescence spectrometers (XRF)

The chemical composition and the silica alumina ( $\text{SiO}_2/\text{Al}_2\text{O}_3$ ) ratio in a sample were determined by X-ray fluorescence (WDXRF) using a Bruker S8 Tiger spectrometer.

#### 3.2.2.3 Surface area analyzer

The Brunauer-Emmett-Teller (BET) technique was used to determine the specific surface area, pore diameter, and total pore volume of catalysts using the surface area analyzer (Quantachrome, Autosorb-1MP). Before the measurements, the samples were degassed under vacuum at  $250^\circ\text{C}$  for 16 h. Then, the sample was placed in the analysis station and operated with nitrogen gas at  $-196^\circ\text{C}$ .

#### 3.2.2.4 Temperature-programmed desorption/reduction/oxidation analyzer (TPDRO/BELCAT II)

The temperature programmed desorption/reduction/oxidation analyzer (TPDRO), BELCAT II, was employed to determine the acidity from the temperature desorption of ammonia. In a typical procedure, 0.1-0.15 g of the catalyst was pretreated at  $300^\circ\text{C}$  for 1 h under the helium flow ( $30\text{ cm}^3/\text{min}$ ) to remove the adsorbed components. Then, the sample was cooled to  $100^\circ\text{C}$  and saturated with 100% of ammonia gas for 60 min. Subsequently, the sample was flushed with helium gas at  $100^\circ\text{C}$  for 30 min to remove the physisorbed ammonia. Finally, the temperature was ramped from  $100^\circ\text{C}$  to  $800^\circ\text{C}$  at the heating rate of  $10^\circ\text{C}/\text{min}$ , which was held for 30 min at  $800^\circ\text{C}$ , before the evolved ammonia was quantified by using a thermal conductivity detector.

#### 3.2.2.5 Simultaneous thermal analysis

Simultaneous thermal analysis (NETZSCH STA 449F3) was used to estimate an amount of coke. Five milligrams of catalysts were burned to remove moisture by placing into the machine. The sample was heated from  $30^\circ\text{C}$  to  $800^\circ\text{C}$ . Subsequently, the sample was cooled to  $30^\circ\text{C}$ . The mass change between  $250^\circ\text{C}$  -  $600^\circ\text{C}$  was an amount of coke.



### 3.2.3 Catalytic Activity

The catalytic activity of olefins removal from aromatics was tested in a batch-type PARR reactor that was equipped with flow controller and a heating system, as shown in Figure 3.1. The composition of the reaction mixture was 150 ml reformat and 9 g catalyst. The catalytic activity was carried out with the stirring rate of 30 rpm at 195°C for 6 h under 12 barg. The liquid product was analyzed for its composition using the bromine index analyzer.



**Figure 3.1** Parr reactor.

### 3.2.4 Product Analysis

The Liquid products were collected at 30 min, 1 h, 1.5 h, 2 h, 3 h, and 6 h of the reaction time. The samples were analyzed using a bromine index analyzer (Titrand 851 Metrohm), as shown in Figure 3.2.

When a sample was injected into the injection port, bromine, which are generated from electrode, reacted with olefins in the sample until titration reached at the end point. Bromine index and olefins conversion were calculated from Equation 3.1 and 3.2, respectively.



**Figure 3.2** Bromine index analyzer.

$$\text{Bromine index(mg/100 g sample)} = \frac{\text{EP} \times 0.1}{\text{Sample size}} \quad (3.1)$$

EP = Bromine, which was produced to reach the end point

0.1 = Calculation factor mg/100 g

$$\text{Olefins removal (\%)} = \frac{\text{BI}_0 - \text{BI}}{\text{BI}_0} \times 100 \% \quad (3.2)$$

BI<sub>0</sub> = Bromine index of raw aromatic hydrocarbon

BI = Bromine index of product

## CHAPTER 4

### RESULTS AND DISCUSSION

In this chapter, the catalytic activity of olefins removal from aromatics in alkylation reaction was investigated. The olefins removal of catalysts was determined by a bromine index. In addition, the properties of catalysts were characterized by x-ray diffraction (XRD), x-ray fluorescence (XRF), Brunauer-Emmett-Teller surface area analyzer (BET), temperature programmed desorption (TPD), and simultaneous thermal analyzer (STA). There are two groups of solid acid catalysts used in this work, zeolites and clays. In section 4.1, various zeolites were screened in order to select a suitable zeolite for modification. The selected zeolite was then modified by dealumination with citric acid in order to enhance the performance of zeolite. The properties and catalytic activity of modified zeolite with citric acid were discussed in section 4.2. Similarly with zeolites, in section 4.3, various clays were screened in order to select a suitable clay for modification by acid activation with hydrochloric acid. The properties and catalytic activity of modified clay with hydrochloric acid were discussed in section 4.4. Finally, section 4.5 compares the catalytic activity of olefins removal between modified zeolite and modified clay. Moreover, advantages and disadvantages of zeolite and clay were considered in this section.

#### 4.1 Zeolites

MCM-22, beta, USY, and mordenite were used in this study. In order to select suitable zeolites for alkylation reaction. MCM-22, beta, USY, and mordenite were screened by considering their catalytic activity and cost. Details of properties and catalytic activity of zeolites were discussed in sections 4.1.1 and 4.1.2, respectively.

#### 4.1.1 Properties of Zeolites

MCM-22, beta, USY, and mordenite are a large pore size group of zeolites, which have different structures. The silica to alumina ratio ( $\text{SiO}_2/\text{Al}_2\text{O}_3$ ) plays an important role on the properties of zeolites, especially the number of acid sites and acid strength. For the same type of zeolite, an increase in the silica to alumina ratio results in a decrease in the number of acid sites, but an increase in the acid strength. The silica to alumina ratio of zeolites was determined by x-ray fluorescence (XRF). The silica to alumina ratio of MCM-22, beta, USY, and mordenite are 30, 22, 7, and 17, respectively, as shown in Table 4.1.

**Table 4.1** Silica to alumina ratio ( $\text{SiO}_2/\text{Al}_2\text{O}_3$ ) of MCM-22, beta, USY, and mordenite

| Sample    | $\text{SiO}_2/\text{Al}_2\text{O}_3$ ratio |
|-----------|--|
| MCM-22    | 30   |
| Beta      | 22   |
| USY       | 7  |
| Mordenite | 17   |

The specific surface area and average pore size of zeolites were obtained from the Brunauer-Emmett-Teller surface area analyzer (BET). Table 4.2 summarizes the surface area and average pore size of zeolites. The surface areas of MCM-22, beta, USY, and mordenite are 504, 508, 556, and 395  $\text{m}^2/\text{g}$ , respectively. The average pore sizes of MCM-22, beta, USY, and mordenite are 1.4, 1.4, 3.8, and 1.4 nm, respectively, indicating that they are categorized as a large pore size group of zeolites. In addition, USY exhibits the largest average pore size (3.8 nm) because the structure of USY is three-dimensional 12 ring (Flanigen *et al.*, 2010). In addition, the acidity of zeolites was determined by temperature programmed desorption with ammonia ( $\text{NH}_3$ -TPD). The total acid sites of MCM-22, beta, USY, and mordenite are 1,098, 1,301, 2,056, and 1,555  $\mu\text{mol}/\text{g}$ , respectively, as shown in Table 4.3.

**Table 4.2** Textural properties of MCM-22, beta, USY, and mordenite

| Sample    | Surface area<br>(m <sup>2</sup> /g) <sup>*a</sup> | Average pore size<br>(nm) <sup>*b</sup> |
|-----------|---|---|
| MCM-22    | 504   | 1.40                                    |
| Beta      | 508   | 1.40                                    |
| USY       | 556   | 3.80                                    |
| Mordenite | 395   | 1.40                                    |

\*a calculated from multipoint BET.

\*b calculated from BJH desorption.

**Table 4.3** Acidity of MCM-22, beta, USY, and mordenite

| Sample    | Weak acid sites<br>( $\mu\text{mol/g}$ ) | Strong acid sites<br>( $\mu\text{mol/g}$ ) | Total acid sites<br>( $\mu\text{mol/g}$ ) |
|-----------|--|--|---|
| MCM-22    | 610                                      | 488  | 1,098                                     |
| Beta      | 594                                      | 707  | 1,301                                     |
| USY       | 1,124                                    | 932  | 2,056                                     |
| Mordenite | 856                                      | 699  | 1,555                                     |

#### 4.1.2 Catalytic Activity of Zeolites

In order to investigate the catalytic activity of the zeolites on the olefins removal from aromatics with alkylation reaction, MCM-22, beta, USY, and mordenite were tested in the batch reactor (Parr reactor) at 195 °C and 12 barg for 6 h. The feed used in the reaction is heavy reformat, which has an approximate bromine index of 700 mg/100g sample. At the start of the experiment, the reaction temperature was increased from the room temperature to the desired operating temperature within 35 min.

Figure 4.1 presents the olefins removal from aromatics with alkylation reaction by MCM-22, beta, USY, and mordenite. At the first hour of the reaction, the olefins removal of all zeolites drastically increases because the reaction temperature

increases rapidly to the operating temperature (195 °C). Therefore, this experiment shows the results of initial olefins removal (at 1.5 h reaction time) or how fast of olefins removal and final olefins removal (at 6 h reaction time) or the performance of olefins removal for each zeolite.

The initial olefins removals of MCM-22, beta, USY, and mordenite are 82, 82, 76, and 77%, respectively. The final olefins removals of MCM-22, beta, USY, and mordenite are 87, 87, 84, and 86%, respectively, as shown in Table 4.4. From the results, the initial olefins removal of MCM-22 and beta are similar, which is slightly higher than USY and mordenite, but the final olefins removal of all zeolites is insignificantly different. In addition, the olefins removal does not depend on the total acidity of zeolites. However, the cost of USY is the cheapest one compared with MCM-22, beta, and mordenite. Therefore, USY will be selected for modification by dealumination with citric acid in section 4.2.

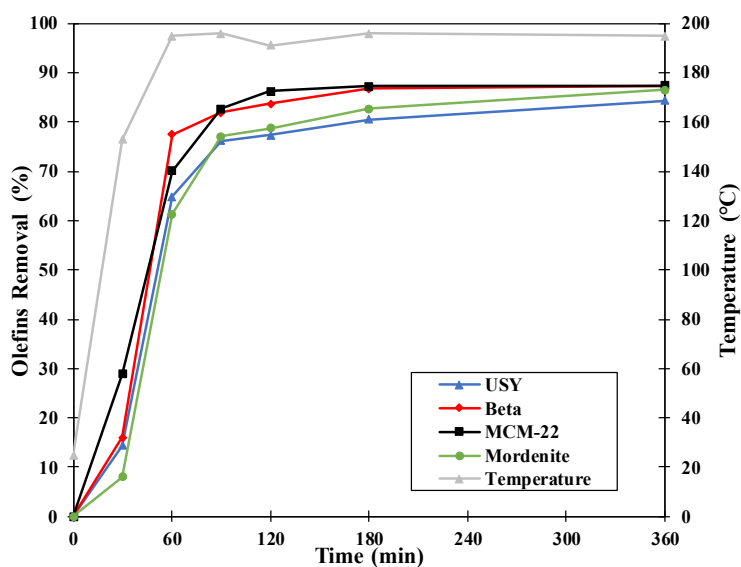


**Figure 4.1** Olefins removal from aromatics in alkylation reaction by MCM-22, beta, USY, and mordenite at 195 °C and 12 barg for 6 h.

**Table 4.4** Initial and final olefins removal by MCM-22, beta, USY, and mordenite

| Sample    | Initial olefins removal (%) | Final olefins removal (%) |
|-----------|-----------------------------|---------------------------|
| MCM-22    | 82                          | 87                        |
| Beta      | 82                          | 87                        |
| USY       | 76                          | 84                        |
| Mordenite | 77                          | 86                        |

#### 4.2 USY Modified by Dealumination with Citric Acid

USY was modified by dealumination with 0.075, 0.15, and 0.3 M citric acid. The properties of USY and modified USY were characterized by x-ray diffraction (XRD), x-ray fluorescence (XRF), Brunauer-Emmett-Teller surface area analyzer (BET), and temperature programmed desorption (TPD), as discussed in section 4.2.1. In addition, the catalytic activity of USY and modified USY was mentioned in section 4.2.2. Finally, in section 4.2.3, the spent catalysts were analyzed for the amount of coke by simultaneous thermal analyzer (STA).

##### 4.2.1 Characteristics of USY and Modified USY

The chemical composition and silica and alumina ratio ( $\text{SiO}_2/\text{Al}_2\text{O}_3$ ) of the USY and USY modified with citric acid were determined by x-ray fluorescence (XRF). Table 4.5 presents the silica to alumina ratio ( $\text{SiO}_2/\text{Al}_2\text{O}_3$ ) and the amount of aluminum ( $\text{Al}_2\text{O}_3$ ) of USY and modified USY by dealumination with 0.075 – 0.3 M citric acid. From the results, the amounts of aluminum of USY, USY-0.075, USY-0.15, and USY-0.3 are 19, 14, 12, and 10 wt%, respectively, while the amount of silica does not change resulting in the increase in the silica to alumina ratio ( $\text{SiO}_2/\text{Al}_2\text{O}_3$ ), which is 7, 9, 11, and 14 for USY, USY-0.075, USY-0.15, and USY-0.3, respectively. The increase in the ratio is due to aluminum leaching from the framework of USY by citric acid.

**Table 4.5** Chemical compositions and crystallinity of USY and USY modified with citric acid

| Sample    | SiO <sub>2</sub> /Al <sub>2</sub> O <sub>3</sub> ratio | Crystallinity (%) | Al <sub>2</sub> O <sub>3</sub> (wt%) |
|-----------|--|-------------------|--------------------------------------|
| USY       | 7  | 100               | 19                                   |
| USY-0.075 | 9  | 98                | 14                                   |
| USY-0.15  | 11   | 91                | 12                                   |
| USY-0.3   | 14   | 81                | 10                                   |

Figure 4.2 presents the XRD patterns of USY and modified USY obtained by dealumination with 0.075, 0.15, and 0.3 M citric acid. The relative crystallinities of the USY and USY modified with citric acid were calculated from the intensity of the characteristic peaks at  $2\theta$  of 11.9, 15.7, 18.7, 20.4, 23.7, 27.1, and 31.4. The percentages of relative crystallinity of USY, USY-0.075, USY-0.15, and USY-0.3 are 100, 98, 91, and 81%, respectively, as shown in Table 4.5. The relative crystallinity of modified USY decreases with the increase in the concentration of citric acid, implying that the crystal structure of modified USY is destroyed by aluminum leaching out from the framework. Therefore, using higher citric acid concentration leads to the collapse of the USY structure. However, the peaks of USY and modified USY are similar, which can be inferred that the extraframework of aluminum (EFAl) presents in the form of amorphous material (Pu *et al.*, 2015).



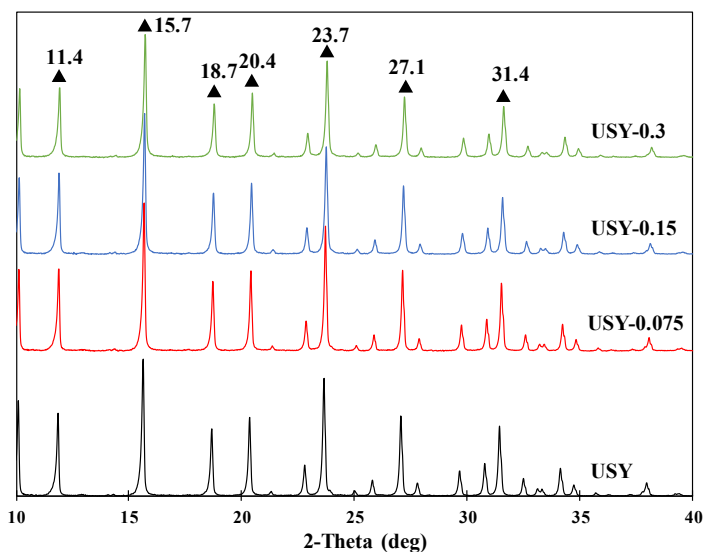


**Figure 4.2** XRD patterns of USY and USY modified with 0.075, 0.15, and 0.3 M citric acid.

The isotherms of nitrogen adsorption of USY and USY modified with citric acid are shown in Figure 4.3. The isotherms of nitrogen adsorption and desorption in both USY and modified USY are similar to type IV, which has a distinct hysteresis loop. The hysteresis loop is the presence of mesopore with the capillary condensation of liquid nitrogen on its surface (Pu *et al.*, 2015). However, the region below hysteresis loop is the micropore. Figure 4.3 illustrates that the increase in the citric concentration from 0.075 – 0.3 M tends to increase the amount of nitrogen adsorption. It indicates that higher citric acid concentration of modified USY results in the increase in the pore volume. Moreover, the pore size distribution of USY and modified USY are shown in Figure 4.4. Table 4.6 shows that the pore volumes of USY, USY-0.075, USY-0.15, and USY-0.3 are 0.09, 0.139, 0.162, and 0.19  $\text{cm}^3/\text{g}$ , respectively. The surface areas of USY, USY-0.075, USY-0.15, and USY-0.3 are 556, 730, 780, and 895  $\text{m}^2/\text{g}$ , respectively. From the results, the average pore sizes of USY and modified USY are similar (3.8 nm), but the pore volume and surface area in both micropore and mesopore areas of modified USY are higher than the USY. It indicates that the micropore and mesopore are effectively generated during the dealumination with citric acid by leaching out aluminum framework in the structure of USY from the



outer to the inner surface (Xin-Mei and Zi-Feng, 2001). Therefore, the USY modified by dealumination with citric acid increases the surface area and pore volume in the parts of micropore and mesopore.

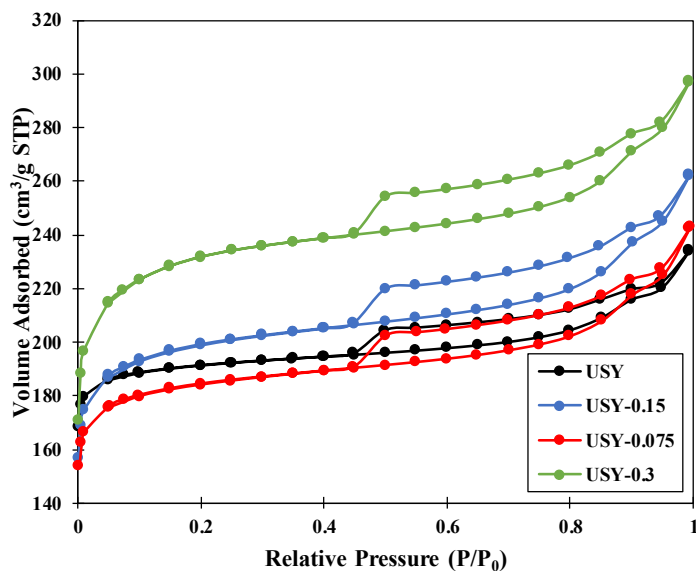


**Figure 4.3** Isotherms of nitrogen adsorption of USY and USY modified with 0.075, 0.15, and 0.3 M citric acid.

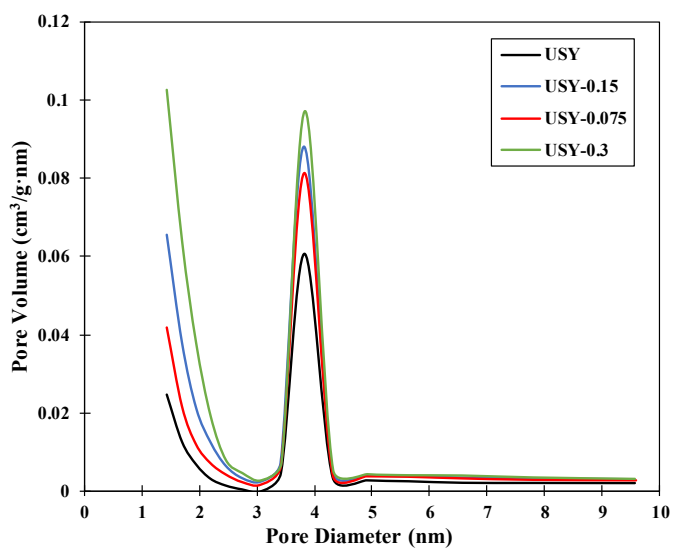


**Figure 4.4** Pore size distribution of USY and USY modified with 0.075, 0.15, and 0.3 M citric acid.

**Table 4.6** Surface area and pore distribution of USY and USY modified with citric acid

| Sample    | Surface area<br>(m <sup>2</sup> /g) <sup>*a</sup> | Pore volume<br>(cm <sup>3</sup> /g) <sup>*b</sup> | Micropore area<br>(m <sup>2</sup> /g) <sup>*c</sup> | Mesopore area<br>(cm <sup>3</sup> /g) <sup>*d</sup> |
|-----------|---|---|---|---|
| USY       | 556   | 0.09  | 501   | 55  |
| USY-0.075 | 730   | 0.139   | 647   | 83  |
| USY-0.15  | 780   | 0.162   | 664   | 116   |
| USY-0.3   | 895   | 0.19  | 735   | 160   |

\*a calculated from multipoint BET.

\*b calculated from BJH desorption.

\*c calculated from t-plot method.

\*d calculated from surface area – micropore area.

The acidity of USY and USY modified with citric acid was characterized by temperature programmed desorption with ammonia (NH<sub>3</sub>-TPD), as shown in Figure 4.5. Table 4.7 shows the weak, strong, and total acid sites of USY and USY modified with different citric acid concentrations. The peaks below 200 °C in the USY and modified USY are due to the desorption of ammonia at low temperature, which exhibits weak acid sites. On the other hand, the peak around 430 °C exhibits strong acid sites. The total acid sites of USY, USY-0.075, USY-0.15, and USY-0.3 are 2,056, 1,729, 1,745, and 1,343 μmol/g, respectively. The results demonstrate that the modification with citric acid decreases the total acid sites of the USY, especially the weak acid sites, leading to the increase in the proportion of strong to total acid sites. That is again due to aluminum leaching from the structure of USY resulting in the increase in the silica to alumina ratio (Xin-Mei and Zi-Feng, 2001).

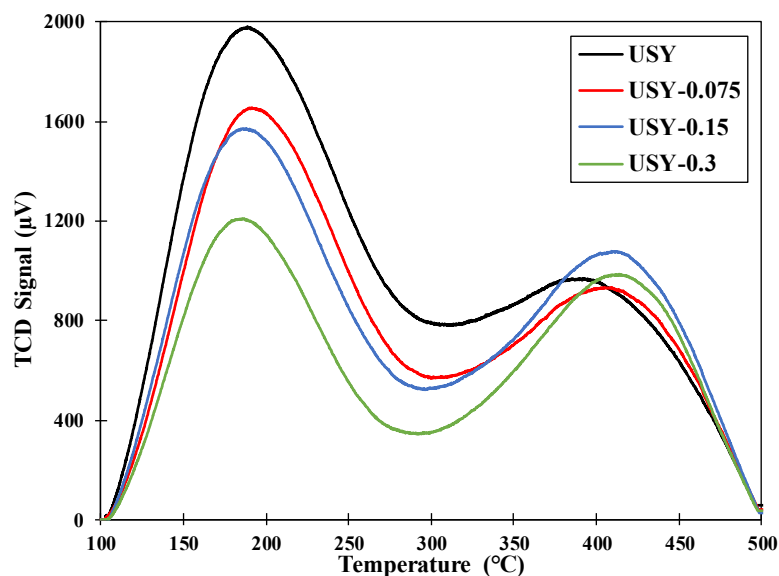


**Figure 4.5** NH<sub>3</sub>-TPD analysis of USY and USY modified with 0.075, 0.15, and 0.3 M citric acid.

**Table 4.7** Acidity of USY and USY modified with citric acid

| Sample    | Weak acid sites<br>( $\mu\text{mol/g}$ ) | Strong acid sites<br>( $\mu\text{mol/g}$ ) | Total acid sites<br>( $\mu\text{mol/g}$ ) |
|-----------|--|--|---|
| USY       | 1,124                                    | 932  | 2,056                                     |
| USY-0.075 | 947                                      | 782  | 1,729                                     |
| USY-0.15  | 921                                      | 824  | 1,745                                     |
| USY-0.3   | 657                                      | 686  | 1,343                                     |

#### 4.2.2 Catalytic Activity of Modified USY

In this section, the catalytic activity of USY and USY modified by dealumination with citric acid for olefins removal from aromatics with alkylation reaction are considered. Figure 4.6 presents olefins removal from aromatics in the alkylation reaction of USY and modified USY, both initial (at 1.5 reaction time h) and final olefins removal (at 6 h reaction time). Table 4.8 shows the initial and final olefins conversion of USY and modified USY. The initial olefins removals of USY, USY-0.075, USY-0.15, and USY-0.3 are 76, 81, 87, and 87%, respectively. The final

olefins removals of USY, USY-0.075, USY-0.15, and USY-0.3 are 84, 86, 90, and 88%, respectively.

Considering the olefins removal of USY and USY modified with citric acid, the modified USY increases the olefins removal because of the increase in the surface area, both micropores and mesopores, leading to enhance the activity of olefins removal from aromatics in alkylation reaction. Normally, the olefins removal from aromatics with alkylation reaction mainly occurs in the micropores, but alkylation reaction has some large aromatic molecules ( $C_8^+$ ), which occurs in the mesopores. In addition, the USY modified with citric acid also increases the proportion of strong to total acid sites resulting in the increased olefins removal, especially the initial olefins removal. Therefore, it can be concluded that the dealumination with citric acid enhances the catalytic activity of olefins removal from aromatics in alkylation reaction. However, the olefins removals of USY-0.15 and USY-0.3 are similar in both initial and final olefins removal. Consequently, the USY modified with 0.15 M citric acid has higher potential than the USY modified with 0.3 M because of the low citric acid concentration involved.

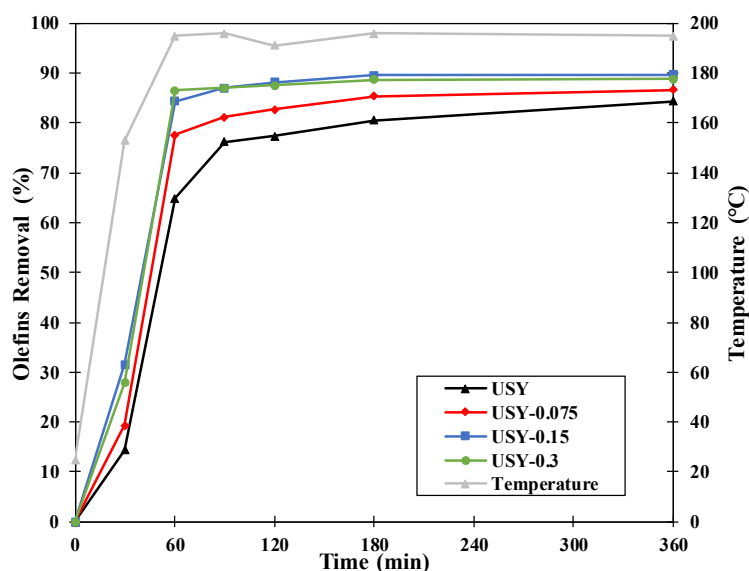


**Figure 4.6** Olefins removal from aromatics in alkylation reaction by USY and USY modified with citric acid at 195 °C and 12 barg for 6 h.

**Table 4.8** Initial and final olefins removal by USY and USY modified with citric acid

| Sample    | Initial olefins removal (%) | Final olefins removal (%) |
|-----------|-----------------------------|---------------------------|
| USY       | 76                          | 84                        |
| USY-0.075 | 81                          | 86                        |
| USY-0.15  | 87                          | 90                        |
| USY-0.3   | 87                          | 88                        |

#### 4.2.3 Deactivation of USY and Modified USY

The main cause of deactivation in the catalytic alkylation for olefins removal from aromatics is coke. Coke is aggregated during the alkylation reaction to block the active sites in the acid catalyst. The temperatures required to burn coke depend on types of coke. Normally, there are two types of coke. First, coke, which is burned at low temperature ( $>250\text{ }^{\circ}\text{C}$ ), is called soft coke. Second, coke, which is burned at high temperature ( $<700\text{ }^{\circ}\text{C}$ ), is called hard coke. Therefore, in order to comprehend the amount of coke, the burning temperature range for estimating the amount of coke is  $250\text{ }^{\circ}\text{C}$  to  $700\text{ }^{\circ}\text{C}$  (Mukarakate *et al.*, 2014).

In this study, the amount of coke deposition was characterized by simultaneous thermal analyzer (STA). Therefore, in this section, spent USY and spent USY modified with 0.15 M citric acid were analyzed to estimate the amount of coke. Figure 4.7 illustrates the mass change (wt%) of spent USY and USY modified with 0.15 M citric acid. It indicates that the amount of coke of spent USY between temperature  $250\text{ }^{\circ}\text{C}$  to  $700\text{ }^{\circ}\text{C}$  is 5.7 wt%, which it is lower than the spent USY modified with 0.15 M citric acid (6.9 wt%) because the modified USY has higher proportion of strong to total acid sites.

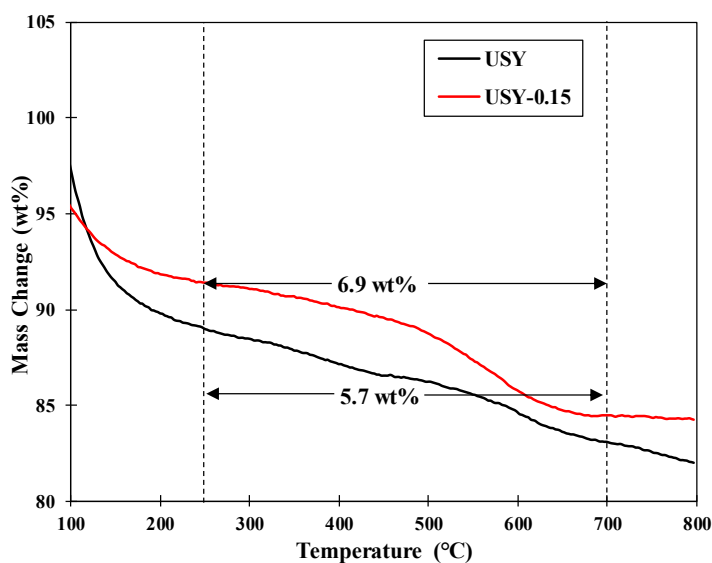


**Figure 4.7** Mass change of spent USY and USY modified with 0.15 M citric acid.

### 4.3 Clays

Illite, bentonite, and bleaching earth were used in this experiment to study the catalytic activity of catalysts in alkylation reaction. In order to select suitable clays for alkylation reaction. Illite, bentonite, and bleaching earth were screened by considering their catalytic activity and cost. Details of properties and catalytic activity of clays were discussed in sections 4.3.1 and 4.3.2, respectively.

#### 4.3.1 Properties of Clays

Illite, bentonite, and bleaching earth are 2:1 layered dioctahedral aluminosilicate. Normally, the interlayer of bentonite and bleaching earth always mainly contain water molecule and a little of cation, which is called swelling clay. However, the interlayer of illite is abundant with potassium oxide, which it is called non-expanding clay. Therefore, clay minerals on aluminosilicate sheets and interlayer of clay affect physicochemical properties, i.e., interlayer space, surface area, and cation exchange (Dutta, 2018).

The chemical compositions of clays were determined by x-ray fluorescence (XRF). Table 4.9 presents the clay minerals of illite, bentonite, and

bleaching earth. From the table, illite, bentonite, and bleaching earth compose of aluminosilicate and metal cation as an impurity, i.e., potassium oxide, iron(III) oxide, magnesium oxide, etc. The silica to alumina ratios ( $\text{SiO}_2/\text{Al}_2\text{O}_3$ ) of illite, bentonite, and bleaching earth are approximately 4, 5, and 6, respectively. In addition, potassium oxide is a mainly metal cation as an impurity in the illite. Therefore, illite is a non-expanding clay. However, the other metal cations, i.e., iron(III) oxide, magnesium oxide, and calcium oxide do not affect to swelling or non-expanding clay.

**Table 4.9** Chemical compositions of illite, bentonite, and bleaching earth

| Sample          | Chemical compositions (wt%) |                                |                  |                                |      |                  |      |                   |                 |                               |
|-----------------|-----------------------------|--------------------------------|------------------|--------------------------------|------|------------------|------|-------------------|-----------------|-------------------------------|
|                 | SiO <sub>2</sub>            | Al <sub>2</sub> O <sub>3</sub> | K <sub>2</sub> O | Fe <sub>2</sub> O <sub>3</sub> | MgO  | TiO <sub>2</sub> | CaO  | Na <sub>2</sub> O | SO <sub>3</sub> | P <sub>2</sub> O <sub>5</sub> |
| Illite          | 66.40                       | 18.30                          | 6.01             | 2.27                           | 1.43 | 0.27             | -    | -                 | -               | -                             |
| Bentonite       | 70.70                       | 15.70                          | 0.74             | 2.94                           | 2.61 | 0.52             | 0.95 | 1.35              | -               | -                             |
| Bleaching earth | 56.5                        | 10.1                           | 2.42             | 10.7                           | 5.02 | 1.42             | 4.81 | -                 | 3.53            | 0.136                         |

The specific surface area and average pore size of clays were obtained from the Brunauer-Emmett-Teller surface area analyzer (BET). Table 4.10 summarizes the textural properties of illite, bentonite, and bleaching earth. The average pore size of illite, bentonite, and bleaching earth are similar (3.8 nm). It indicates that they are mesoporous materials. In addition, the surface areas of illite, bentonite, and bleaching earth are 5.6, 40, and 100 m<sup>2</sup>/g, respectively. Since, illite is a non-expanding clay resulting in the lowest surface area (5.6 m<sup>2</sup>/g) compared with bentonite and bleaching earth, which are swelling clay (Sidorenko *et al.*, 2018). In addition, the acidity of illite, bentonite, and bleaching earth was determined by temperature programmed desorption with ammonia (NH<sub>3</sub>-TPD). Table 4.11 shows that the total acid sites of illite, bentonite, and bleaching earth are 651, 1,531, and 1,954 μmol/g, respectively.



**Table 4.10** Textural properties of clays

| Sample          | Surface area<br>(m <sup>2</sup> /g) <sup>*a</sup> | Average pore size<br>(nm) <sup>*b</sup> |
|-----------------|---|---|
| Illite          | 5.60  | 3.80                                    |
| Bentonite       | 41  | 3.80                                    |
| Bleaching earth | 100   | 3.80                                    |

\*a calculated from multipoint BET.

\*b calculated from BJH desorption.

**Table 4.11** Acidity of illite, bentonite, and bleaching earth

| Sample          | Weak acid sites<br>( $\mu\text{mol/g}$ ) | Strong acid sites<br>( $\mu\text{mol/g}$ ) | Total acid sites<br>( $\mu\text{mol/g}$ ) |
|-----------------|--|--|---|
| Illite          | -  | 651  | 651                                       |
| Bentonite       | 12                                       | 1,519                                      | 1,531                                     |
| Bleaching earth | 983                                      | 971  | 1,954                                     |

#### 4.3.2 Catalytic Activity of Clays

Similar with the zeolites, the catalytic activity of clays on the olefins removal from aromatics with alkylation reaction was investigated. Illite, bentonite, and bleaching earth were tested in the batch reactor (Parr reactor) at 195 °C and 12 barg for 6 h. At the start of the experiment, the reaction temperature was increased from the room temperature to the desired operating temperature within 35 min. Therefore, clays were screened in order to select a suitable clay for modification by acid activation with hydrochloric acid.

Figure 4.8 presents the olefins removal from aromatics with alkylation reaction of illite, bentonite, and bleaching earth. During the first hour of the reaction, the rapid increase of reaction temperature to 195 °C results in the significant increase in the olefins removal. Therefore, in this experiment, the olefins removal at 1.5 h reaction time is the initial olefins removal, which shows how fast of olefins removal

is. On the other hand, the olefins removal at 6 h reaction time is the final olefins removal, which shows the performance of olefins removal for each clay.

Table 4.12 shows initial and final olefins removals of illite, bentonite, and bleaching earth. The initial olefins removals of illite, bentonite, and bleaching earth are 52, 77, and 81%, respectively. The final olefins removals of illite, bentonite, and bleaching earth are 69, 87, and 87%, respectively. From the results, the initial and final olefins removals in both bentonite and bleaching earth are slightly different, but the initial and final olefins removals of bentonite and bleaching earth are higher than illite. Since, the acidity of illite is much lower than bentonite and bleaching earth resulting in the lowest olefins removal of illite. However, the costs of illite and bentonite are inexpensive and cheaper than bleaching earth. Therefore, bentonite was selected for modification by acid activation. The properties and catalytic activity of bentonite and modified bentonite were discussed in section 4.4.

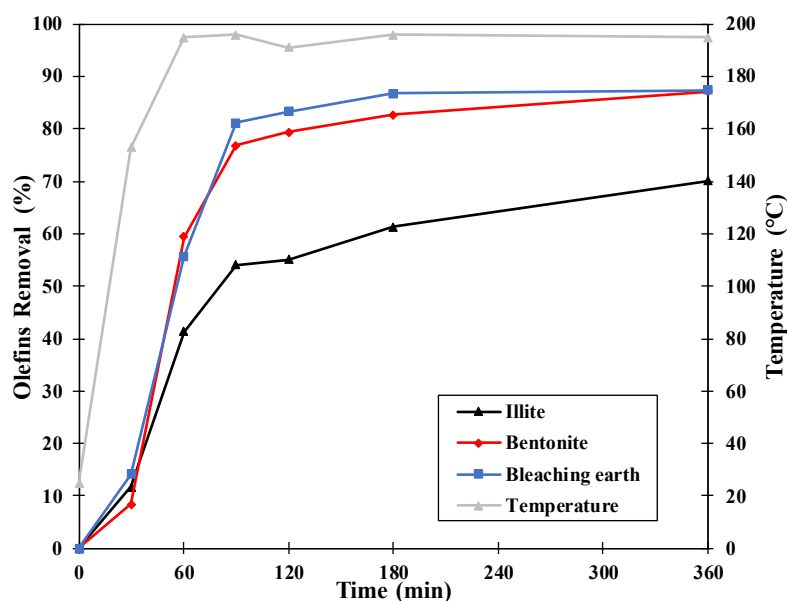


**Figure 4.8** Olefins removal from aromatics in alkylation reaction by illite, bentonite, and bleaching earth at 195 °C and 12 barg for 6 h.

**Table 4.12** Initial and final olefins removal by illite, bentonite, and bleaching earth

| Sample          | Initial olefins removal (%) | Final olefins removal (%) |
|-----------------|-----------------------------|---------------------------|
| Illite          | 52                          | 69                        |
| Bentonite       | 77                          | 87                        |
| Bleaching earth | 81                          | 87                        |

#### 4.4 Bentonite Modified by Acid Activation with Hydrochloric Acid

Bentonite was modified by acid activation with 1, 3, and 6 M hydrochloric acid. The properties of bentonite and modified bentonite were characterized by x-ray diffraction (XRD), x-ray fluorescence (XRF), Brunauer-Emmett-Teller surface area analyzer (BET), and temperature programmed desorption (TPD), as discussed in section 4.4.1. In addition, the catalytic activity of bentonite and modified bentonite was mentioned in section 4.4.2. Finally, in section 4.4.3, the spent catalysts were analyzed for the amount of coke by simultaneous thermal analyzer (STA).

##### 4.4.1 Characteristics of Bentonite and Modified Bentonite

X-ray fluorescence was used to determine the chemical composition of the bentonite and bentonite modified with hydrochloric acid. Table 4.13 and Figure 4.9 summarize the chemical composition and the relative contents of metal oxides ( $M/M_0$ ) of bentonite and bentonite modified with hydrochloric acid, respectively, where  $M_0$  and  $M$  are the mass in percent of element oxides in bentonite and modified bentonite. The contents of  $Fe_2O_3$ ,  $MgO$ ,  $CaO$ ,  $Al_2O_3$ , and  $Na_2O$  decrease after treatment with 1 – 6 M hydrochloric acid. After acid activation with 6 M hydrochloric acid, the  $Fe_2O_3$ ,  $MgO$ ,  $CaO$ , and  $Na_2O$  contents decrease by 23.8%, 54.4%, 60%, and 40.7% respectively. Therefore, it indicates that the acid activation of bentonite with hydrochloric acid removes some metal oxides as impurities. However, the acid activation with hydrochloric acid increases the amount of  $SiO_2$ ,  $K_2O$ , and  $TiO_2$  because these cations are not dissolved by acid activation with hydrochloric acid

resulting in remobilization of these cations. Therefore, the relative contents of undissolved elements, i.e.,  $\text{SiO}_2$ ,  $\text{K}_2\text{O}$ , and  $\text{TiO}_2$  increase (Bergaya *et al.*, 2006).

**Table 4.13** Chemical composition of bentonite and bentonite modified with hydrochloric acid

| Sample    | Chemical compositions (wt%) |                         |                         |              |                       |              |                      |                |
|-----------|-----------------------------|-------------------------|-------------------------|--------------|-----------------------|--------------|----------------------|----------------|
|           | $\text{SiO}_2$              | $\text{Al}_2\text{O}_3$ | $\text{Fe}_2\text{O}_3$ | $\text{MgO}$ | $\text{Na}_2\text{O}$ | $\text{CaO}$ | $\text{K}_2\text{O}$ | $\text{TiO}_2$ |
| Bentonite | 70.70                       | 15.70                   | 2.94                    | 2.61         | 1.35                  | 0.95         | 0.74                 | 0.53           |
| Ben-1     | 74.30                       | 14.50                   | 2.56                    | 1.74         | 0.71                  | 0.56         | 0.83                 | 0.68           |
| Ben-3     | 78.60                       | 12.50                   | 2.29                    | 1.24         | 0.83                  | 0.41         | 0.98                 | 0.69           |
| Ben-6     | 76.90                       | 12.80                   | 2.24                    | 1.19         | 0.80                  | 0.38         | 1.02                 | 0.72           |

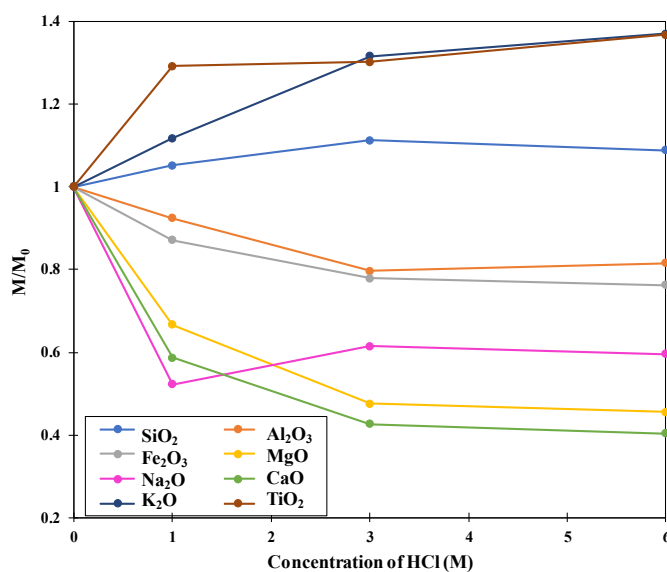


**Figure 4.9** Relative contents of metal oxides ( $M/M_0$ ) of bentonite and bentonite modified with hydrochloric acid.

The x-ray diffraction patterns of bentonite and bentonite modified with hydrochloric acid are given in Figure 4.10. The bentonite and modified bentonite are composed mainly of montmorillonite with characteristic peaks at  $2\theta$  of 5.7 with basal

spacing ( $d_{001}$ ). The other peaks are quartz and feldspars. From the figure, it can be observed that acid attacks the structure of bentonite causing a decrease intensity of first montmorillonite peak ( $2\theta = 5.7$ ) during acid activation with hydrochloric acid. However, hydrochloric acid cannot destroy quartz and feldspars resulting in the peak of quartz and feldspars unchanged (Zhirong *et al.*, 2011).

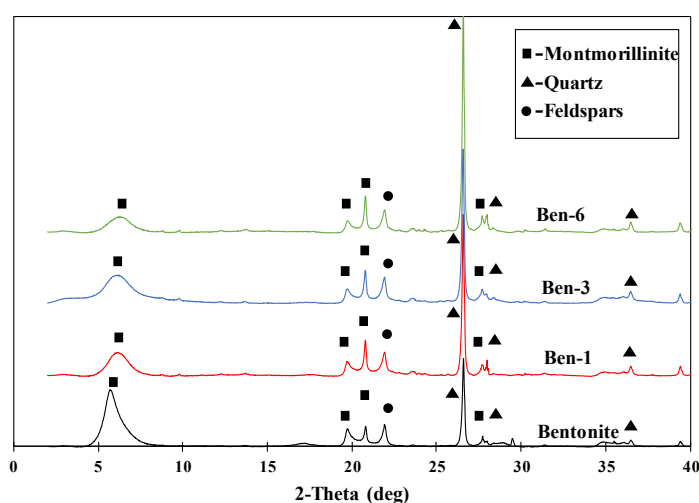


**Figure 4.10** XRD patterns of bentonite and bentonite modified with 1, 3, and 6 M hydrochloric acid.

The isotherms of nitrogen adsorption of bentonite and bentonite modified with hydrochloric acid are shown in Figure 4.11. The isotherms of nitrogen adsorption and desorption, in both bentonite and modified bentonite, are similar to type IV, which has a distinct hysteresis loop. The hysteresis loop is the presence of mesopore with the capillary condensation of liquid nitrogen on its surface, but the region below hysteresis loop is the micropore (Yildiz *et al.*, 2004). From Figure 4.11, the increase in the hydrochloric acid concentration from 1 – 6 M tends to increase the amount of nitrogen adsorption. It means that the increase in the hydrochloric acid concentration in modified bentonite increases the pore volume of the bentonite.

The pore size distributions of bentonite and modified bentonite are shown in Figure 4.11. Table 4.14 shows that the pore volumes of bentonite, ben-1, ben-3, and ben-6 are 0.136, 0.138, 0.14, and 0.19  $\text{cm}^3/\text{g}$ , respectively. The surface

areas of bentonite, ben-1, ben-3, and ben-6 are 40, 41, 46, and 68 m<sup>2</sup>/g, respectively. It is clear that the average pore sizes of bentonite and modified bentonite are similar (3.8 nm), but the pore volume and surface area of modified bentonite are higher than the bentonite. In addition, from Figure 4.12, the main parts of surface areas of bentonite and modified bentonite are mesopore. The increase in the surface area and pore volume during acid activation of bentonite occurs because of the removal of impurities in the structure of bentonite.

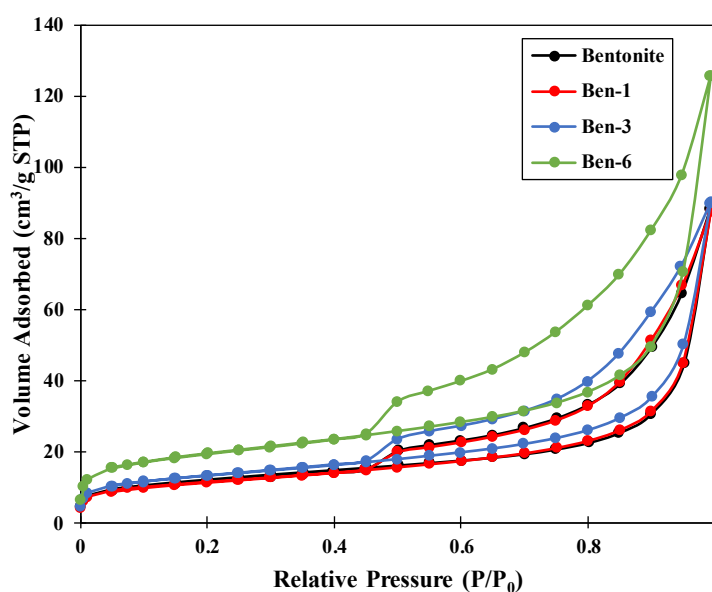


**Figure 4.11** Isotherms of nitrogen adsorption of bentonite and bentonite modified with 1, 3, and 6 M hydrochloric acid.

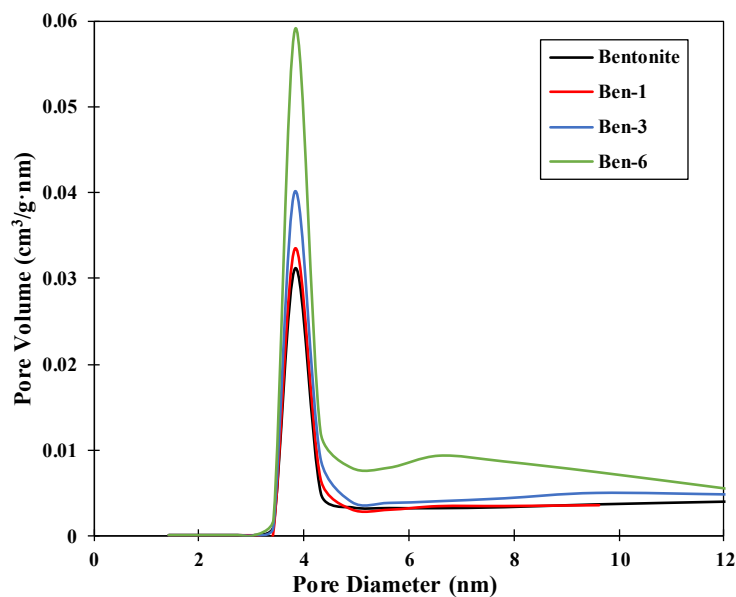


**Figure 4.12** Pore size distribution of bentonite and bentonite modified with 1, 3, and 6 M hydrochloric acid.

**Table 4.14** Surface area and pore distribution of bentonite and bentonite modified with hydrochloric acid

| Sample    | Surface area<br>(m <sup>2</sup> /g) <sup>*a</sup> | Pore volume<br>(cm <sup>3</sup> /g) <sup>*b</sup> | Micropore area<br>(m <sup>2</sup> /g) <sup>*c</sup> | Mesopore area<br>(cm <sup>3</sup> /g) <sup>*d</sup> |
|-----------|---|---|---|---|
| Bentonite | 40  | 0.136   | 5.9   | 34.1  |
| Ben-1     | 41  | 0.138   | 8.8   | 32.2  |
| Ben-3     | 46  | 0.14  | 10  | 36  |
| Ben-6     | 68  | 0.19  | 16.7  | 51.3  |

\*a calculated from multipoint BET.

\*b calculated from BJH desorption.

\*c calculated from t-plot method.

\*d calculated from surface area – micropore area.

Acidity of bentonite and bentonite modified with hydrochloric acid was determined by temperature programmed desorption with ammonia (NH<sub>3</sub>-TPD).

Figure 4.13 illustrates that there are peaks at low temperature (150 °C) and high temperature (650 °C) of ammonia desorption, which are weak and strong acid sites, respectively. Table 4.15 presents weak, strong, and total acid sites of bentonite and bentonite modified with different hydrochloric acid concentrations. The total acid sites of bentonite, ben-1, ben-3, and ben-6 are 1,531, 1,867, 1,588, and 1,279  $\mu\text{mol/g}$ , respectively. The results show that bentonite modified with 1 M hydrochloric acid has the strong acid sites. Normally, negative charge of aluminosilicates layer in bentonite requires cations in the interlayer to balance the charge, which is the source of acidity. However, washing out of impurities with hydrochloric acid in the bentonite structure resulting in the increase in the negative charge. Therefore, the proton intercalates in the interlayer of bentonite to balance the charge leading to the increase in the strong acid sites (Dutta, 2018). However, bentonite modified with 3 and 6 M results in a greater extent in the aluminum leaching out from the structure; hence, the acidity decreases in bentonite.

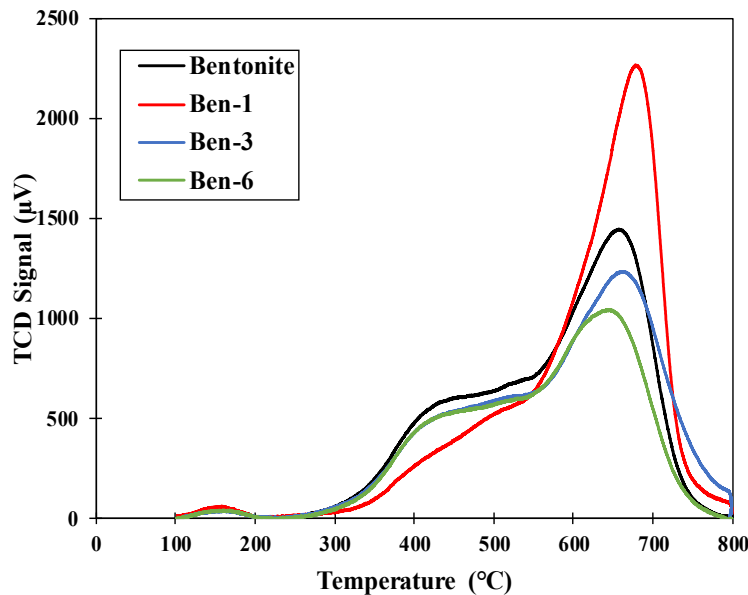


**Figure 4.13** NH<sub>3</sub>-TPD analysis of bentonite and bentonite modified with 1, 3, and 6 M hydrochloric acid.



**Table 4.15** Acidity of bentonite and bentonite modified with hydrochloric acid

| Sample    | Weak acid sites<br>( $\mu\text{mol/g}$ ) | Strong acid sites<br>( $\mu\text{mol/g}$ ) | Total acid sites<br>( $\mu\text{mol/g}$ ) |
|-----------|--|--|---|
| Bentonite | 12                                       | 1,519                                      | 1,531                                     |
| Ben-1     | 17                                       | 1,850                                      | 1,867                                     |
| Ben-3     | 11                                       | 1,577                                      | 1,588                                     |
| Ben-6     | 11                                       | 1,268                                      | 1,279                                     |

#### 4.4.2 Catalytic Activity of Modified Bentonite

In this section, the catalytic activity of bentonite and bentonite modified by acid activation with hydrochloric acid for olefins removal from aromatics with alkylation reaction is considered. Figure 4.14 presents the initial olefins removal (at reaction time 1.5 h) and the final olefins removal (at reaction time 6 h) from the alkylation reaction. The results show that the initial olefins removals of bentonite, Ben-1, Ben-3, and Ben-6 are 74, 81, 78, and 86% respectively. The final olefins removals of bentonite, Ben-1, Ben-3, and Ben-6 are 86, 90, 86, and 85%, respectively, as shown in Table 4.16.

Considering the olefins removal of bentonite and bentonite modified with hydrochloric acid, the bentonite modified with 1 M hydrochloric acid slightly increases the initial and final olefins removal because of the increase in the acidity. However, the olefins removals of bentonite modified with 3 and 6 M hydrochloric acid slightly decrease from the bentonite modified with 1 M hydrochloric acid because of decreasing in the acidity. Therefore, the bentonite modified with 1 M hydrochloric acid has the potential for olefins removal in alkylation reaction.

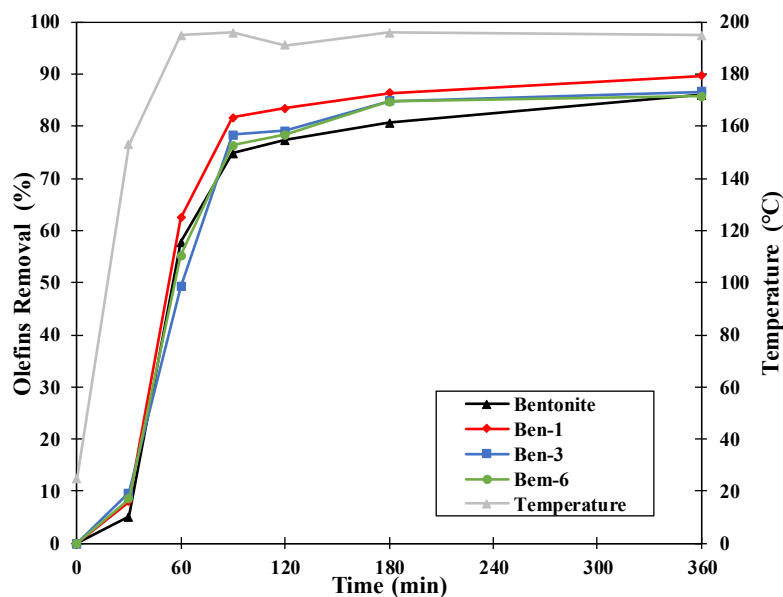


**Figure 4.14** Olefins removal from aromatics in alkylation reaction by bentonite and bentonite modified with hydrochloric acid at 195 °C and 12 barg for 6 h.

**Table 4.16** Initial and final olefins removal by bentonite and bentonite modified with hydrochloric acid

| Sample    | Initial olefins removal (%) | Final olefins removal (%) |
|-----------|-----------------------------|---------------------------|
| Bentonite | 74                          | 86                        |
| Ben-1     | 81                          | 90                        |
| Ben-3     | 78                          | 86                        |
| Ben-6     | 76                          | 85                        |

### 4.3.3 Deactivation of Bentonite and Modified Bentonite

Similar to section 4.1.3, in order to estimate the amounts of coke in bentonite and bentonite modified with hydrochloric acid, spent bentonites were analyzed to estimate the amount of coke by simultaneous thermal analyzer (STA). Figure 4.15 illustrates the mass change (wt%) of spent bentonite and bentonite modified with 1 M hydrochloric acid. It indicates that the amount of coke of spent bentonite between temperature 250 °C to 700 °C is 4.7 wt%, which it is lower than

the spent bentonite modified with 1 M hydrochloric acid (5.5 wt%) because of the increase in the strong acid sites in the modified bentonite.

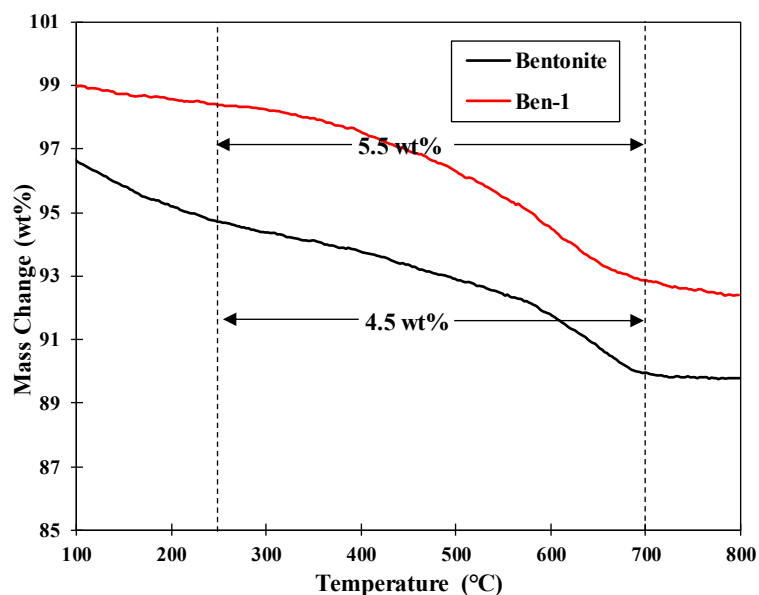


**Figure 4.15** Mass change of spent bentonite and bentonite modified with 1 M hydrochloric acid.

#### 4.5 Comparasion of Modified USY and Modified bentonite

In this section, the properties and catalytic activity of modified USY and modified bentonite were compared. Normally, the structures of USY and bentonite compose of aluminosilicate, but the arrangement of structure in USY and bentonite is different leading to various properties. The framework in the zeolite is a  $TO_4$  tetrahedral, where T-atom is typically Si or Al. However, clays structure are layered aluminosilicate, which composes of tetrahedral layer and octahedral layer.

Table 4.17 presents the properties and final olefins removal of modified USY and modified bentonite. From the table, the surface area of modified USY ( $780 \text{ m}^2/\text{g}$ ) is much higher than modified bentonite ( $41 \text{ m}^2/\text{g}$ ). The total acidity of samples is insignificantly different, but mainly acidity of modified bentonite is strong acid sites, which is different from modified USY. Therefore, in the view point of olefins

removal, the performance of modified USY and modified bentonite for removal of olefins from aromatics in alkylation reaction is similar.

**Table 4.17** Properties and olefins removal of modified USY and modified bentonite

| Sample   | Surface area<br>(m <sup>2</sup> /g) | Acidity<br>( $\mu\text{mol/g}$ ) |                      | Final olefins removal<br>(%) |
|----------|-------------------------------------|----------------------------------|----------------------|------------------------------|
|          |                                     | Weak<br>acid sites               | Strong<br>acid sites |                              |
| USY-0.15 | 780                                 | 921                              | 824                  | 90                           |
| Ben-1    | 41                                  | 17                               | 1,850                | 91                           |



3872731635

## CHAPTER 5

### CONCLUSION AND RECOMMENDATION

#### 5.1 Conclusion

In this work, USY and bentonite were selected for modification to enhance the catalytic activity of olefins removal from aromatic in alkylation reaction. Dealumination of USY modified with 0.15 M citric acid is the suitable condition resulting in suitable proportion of strong acid sites to total acid sites to increase the olefins removal, especially initial olefins removal. The initial and final olefins removal of USY modified with 0.15 M citric acid increase from 76 to 87% and 84 to 90%, respectively. In addition, the acid activation of bentonite modified with 1 M hydrochloric acid increases the total acid sites resulting in the increase in the olefins removal. The increase in the initial and final olefins removal is from 74 to 81% and 86 to 90%, respectively. In the viewpoint of olefins removal, the catalytic activity of USY modified with 0.15 M and bentonite modified with 1 M hydrochloric acid is similar. However, the increase in the strong acid in both of modified USY and modified bentonite increases the amount of coke. The amount of coke of spent modified USY is 6.9 wt%, which is higher than the spent USY (5.7 wt%). The amount of coke of spent modified bentonite is 5.5 wt%, which is higher than the spent bentonite (4.5 wt%).

#### 5.2 Recommendation

In order to select the best catalysts for industry, stability should be tested in a fixed bed reaction. In addition, Bronsted and Lewis acid should be determined by FTIR-pyridine because Bronsted and Lewis acid are parameters affecting the activity and stability.

## APPENDICES

### Appendix A Additional Information

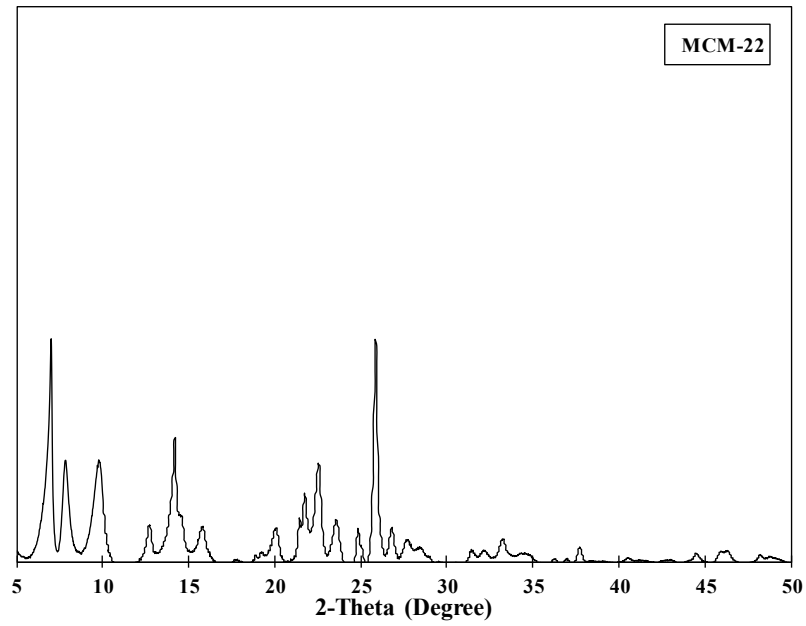


**Figure A1** X-ray diffraction (XRD) of MCM-22.

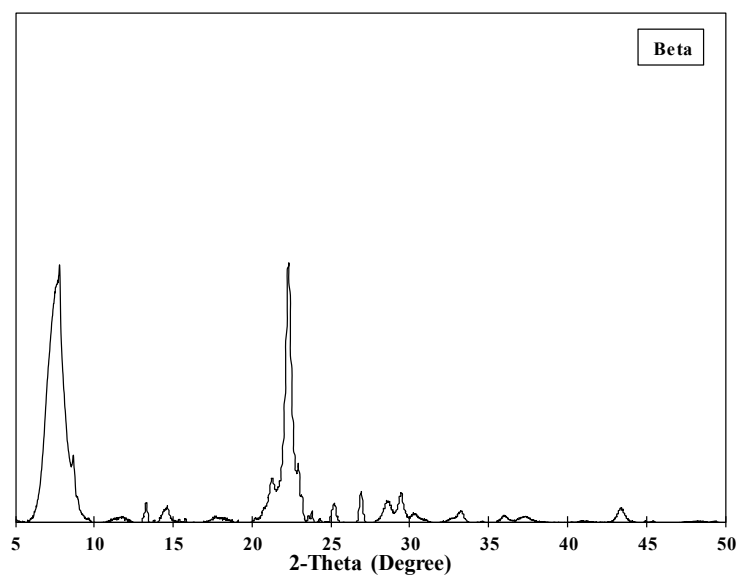


**Figure A2** X-ray diffraction (XRD) of Beta.



3872731635

CU IThesis 6171022063 thesis / rev: 20072563 15:54:37 / seq: 19

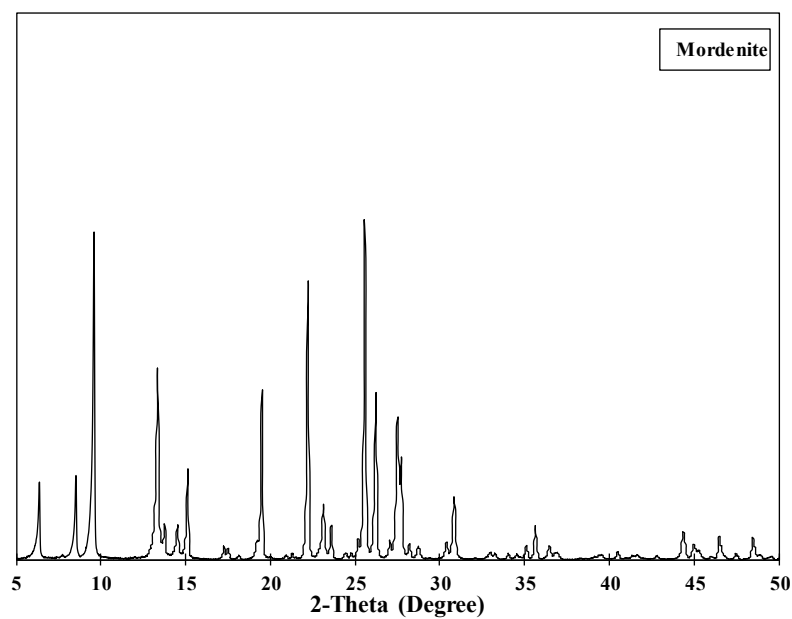


**Figure A3** X-ray diffraction (XRD) of Mordenite.

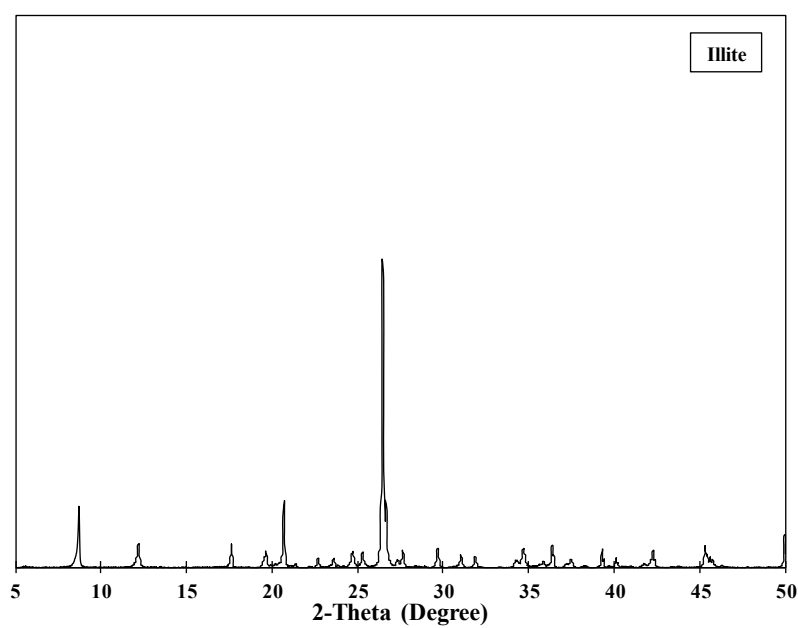


**Figure A4** X-ray diffraction (XRD) of illite.



3872731635

CU IThesis 6171022063 thesis / recv: 20072563 15:54:37 / seq: 19

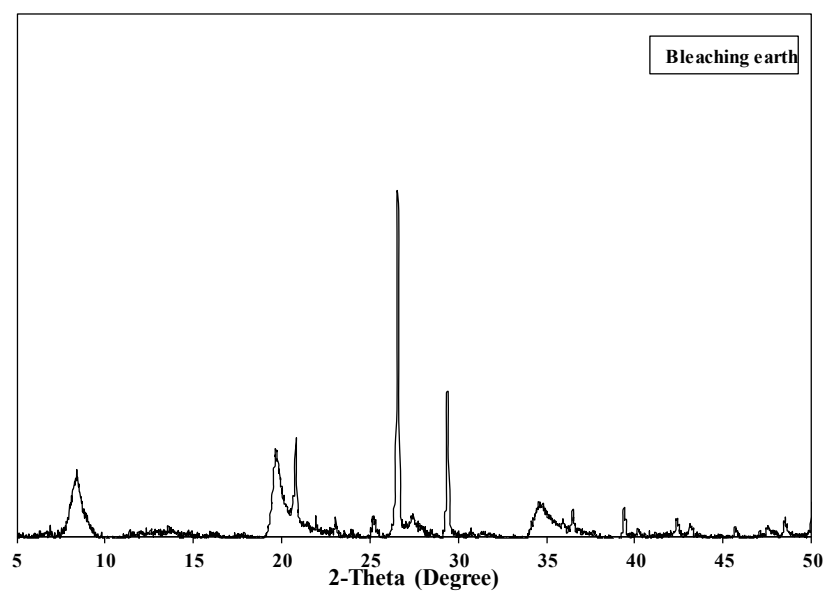


**Figure A5** X-ray diffraction (XRD) of bleaching earth.

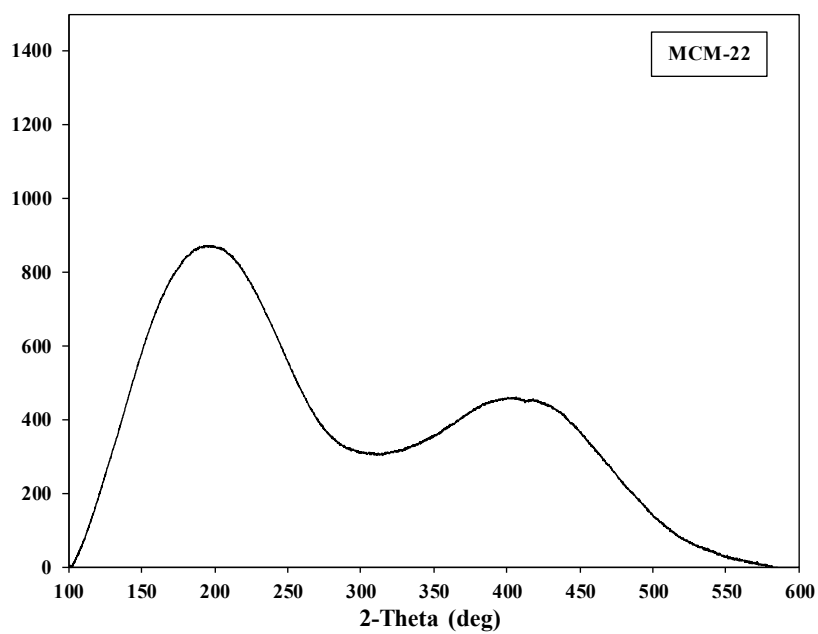


**Figure A6** TPD-NH<sub>3</sub> of MCM-22.



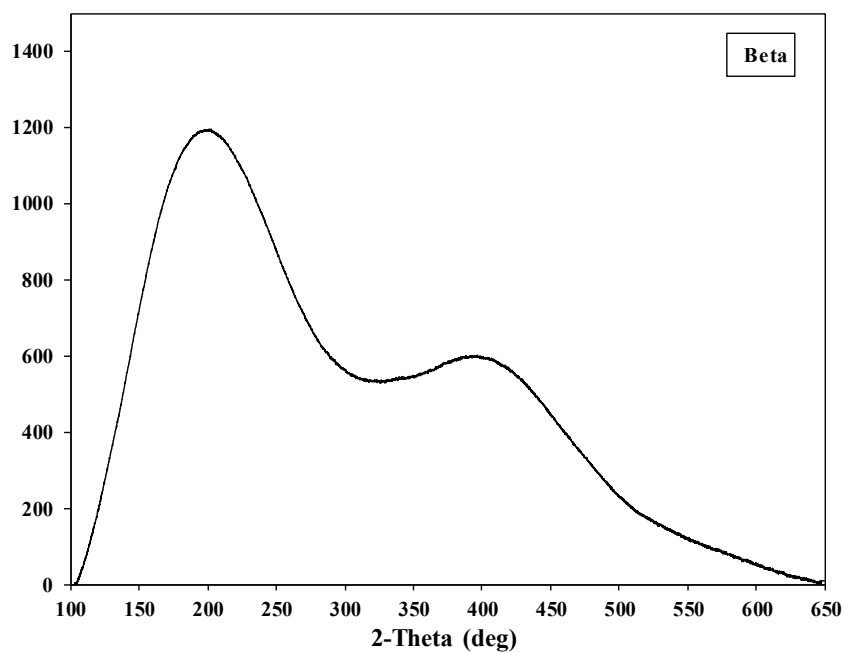


Figure A7 TPD-NH<sub>3</sub> of beta.

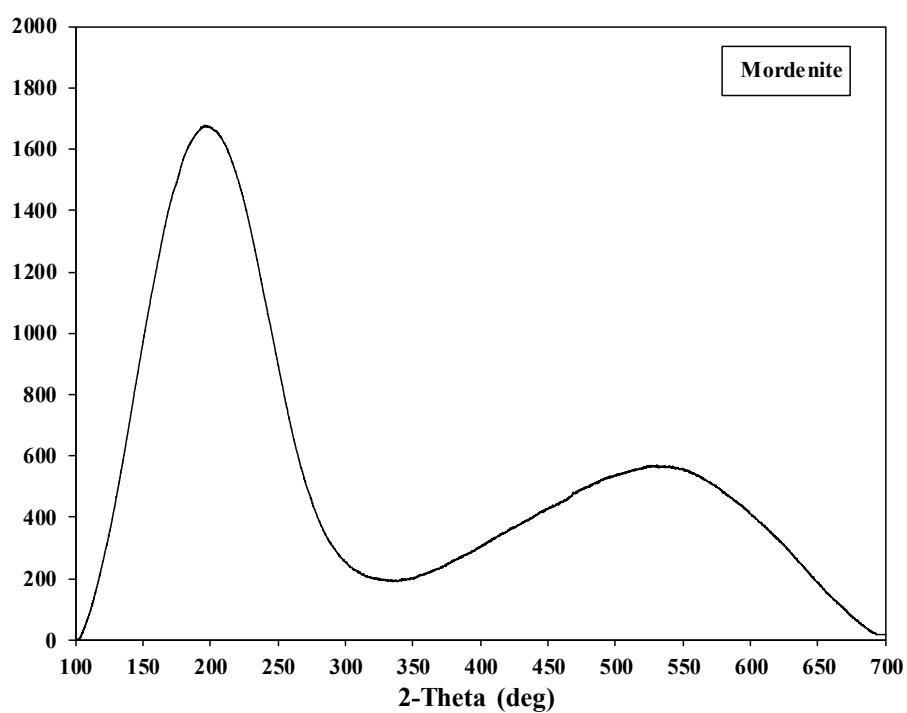
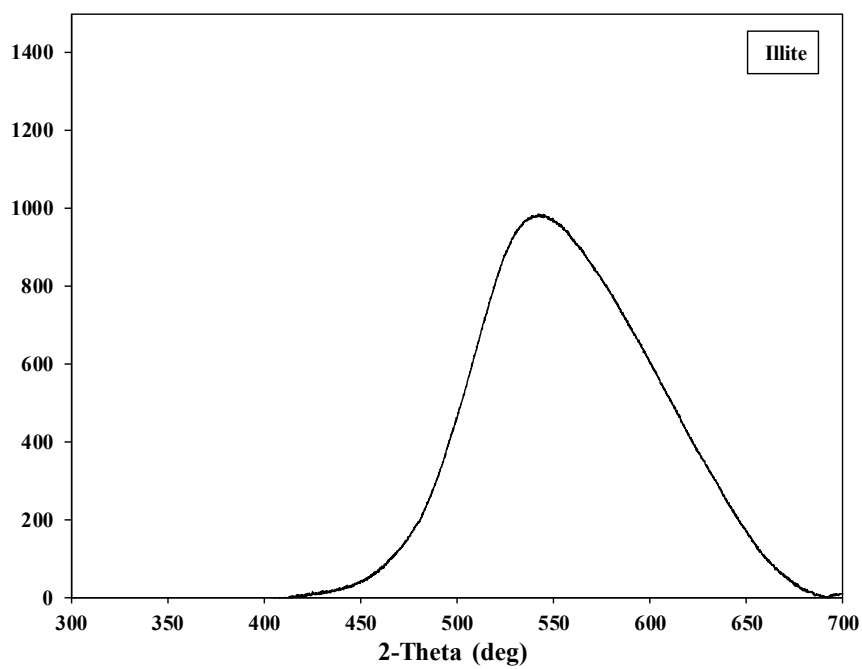


Figure A8 TPD-NH<sub>3</sub> of mordenite.



3872731635

CU Theses 6171022063 thesis / recv: 20072563 15:54:37 / seq: 19



**Figure A9** TPD-NH<sub>3</sub> of illite.

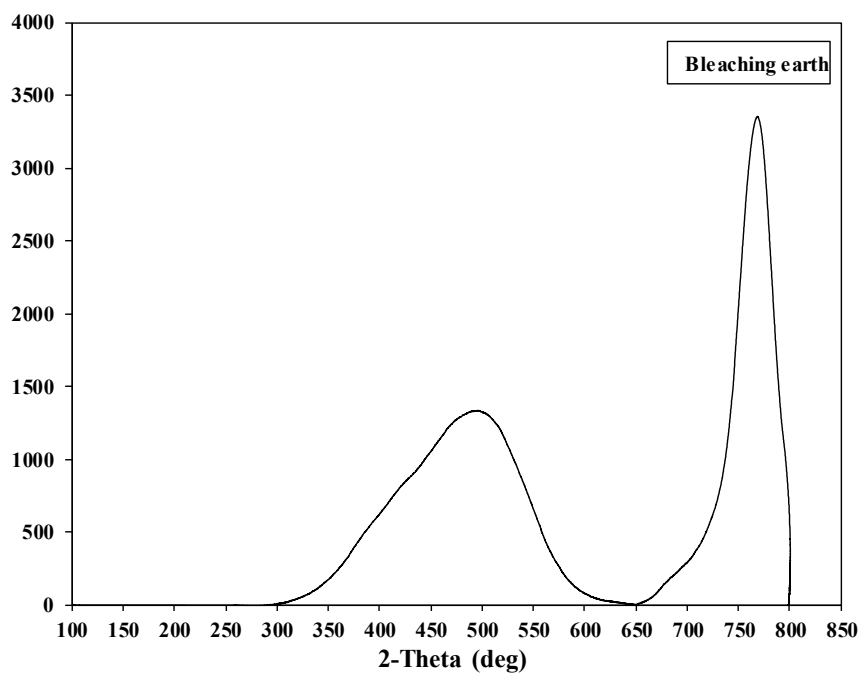


**Figure A10** TPD-NH<sub>3</sub> of bleaching earth.



3872731635

CU Theses 6171022063 thesis / recv: 20072563 15:54:37 / seq: 19

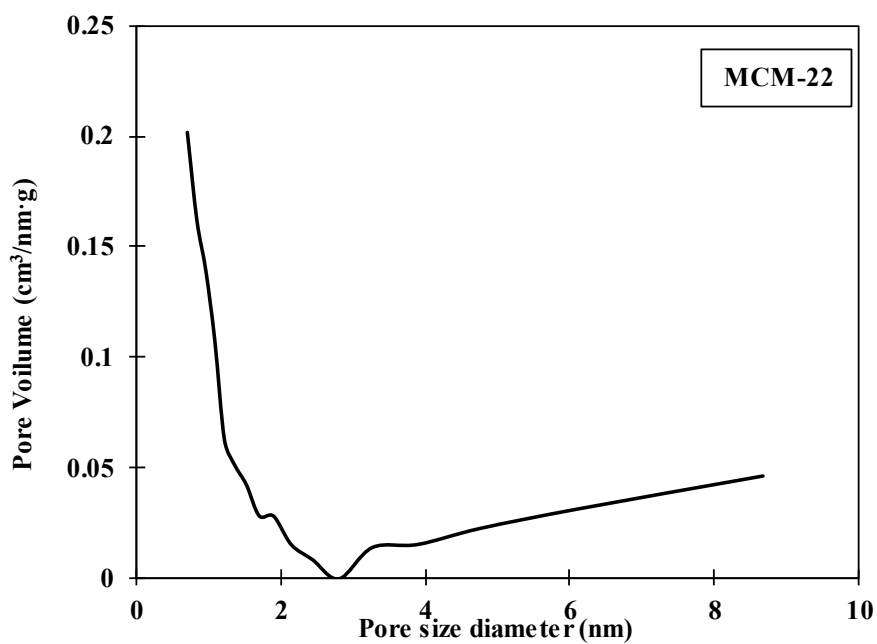


**Figure A11** Pore size distribution of MCM-22.

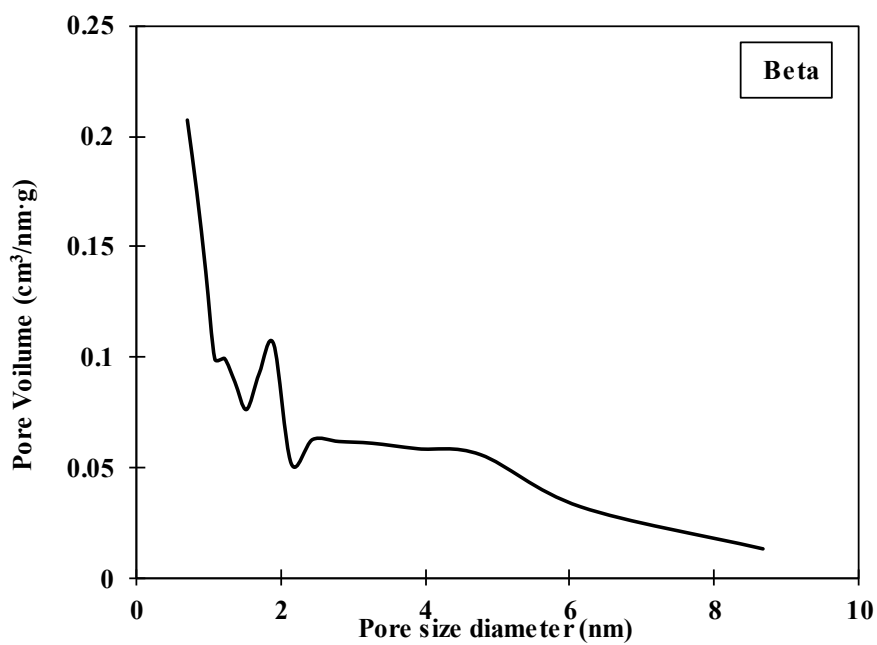


**Figure A12** Pore size distribution of beta.



3872731635

CU Theses 6171022063 thesis / recv: 20072563 15:54:37 / seq: 19

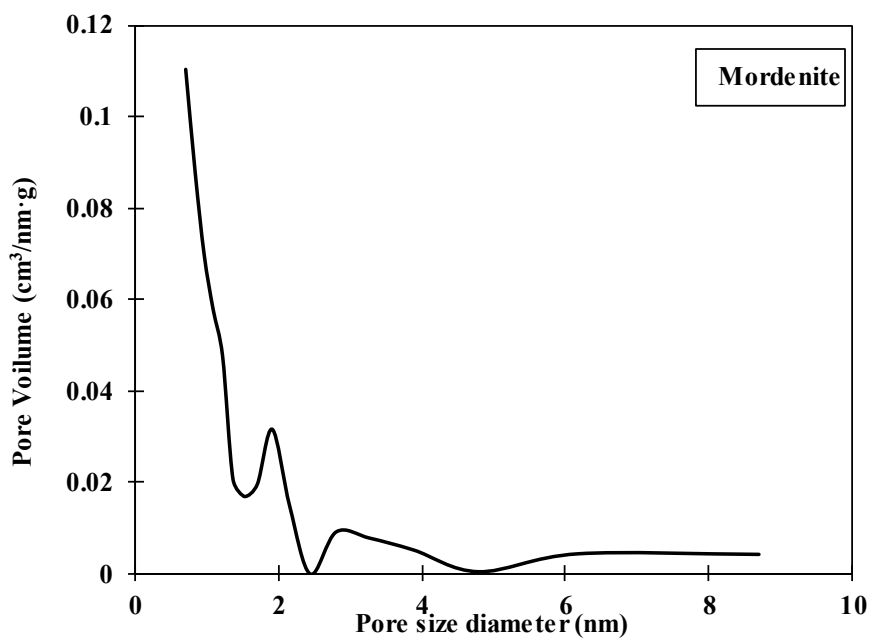


Figure A13 Pore size distribution of mordenite.

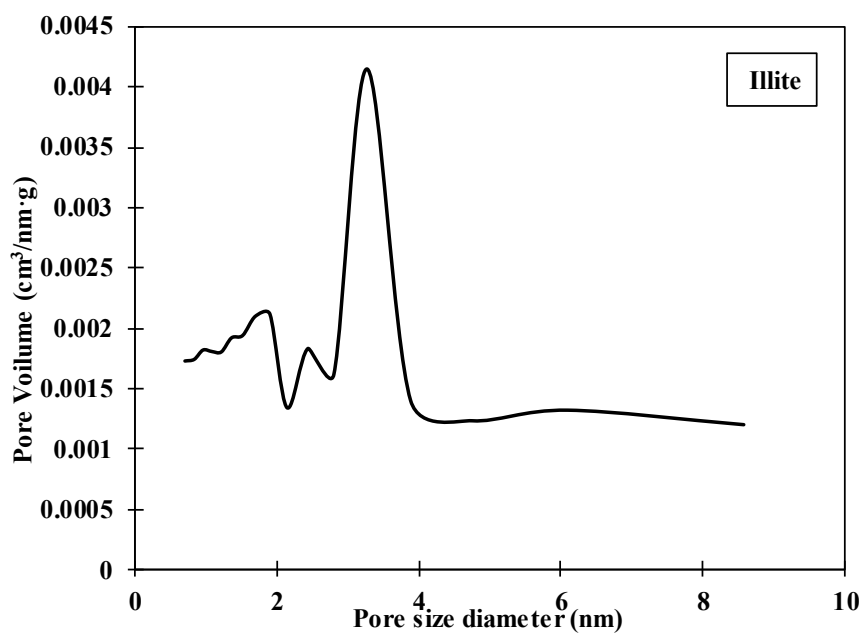
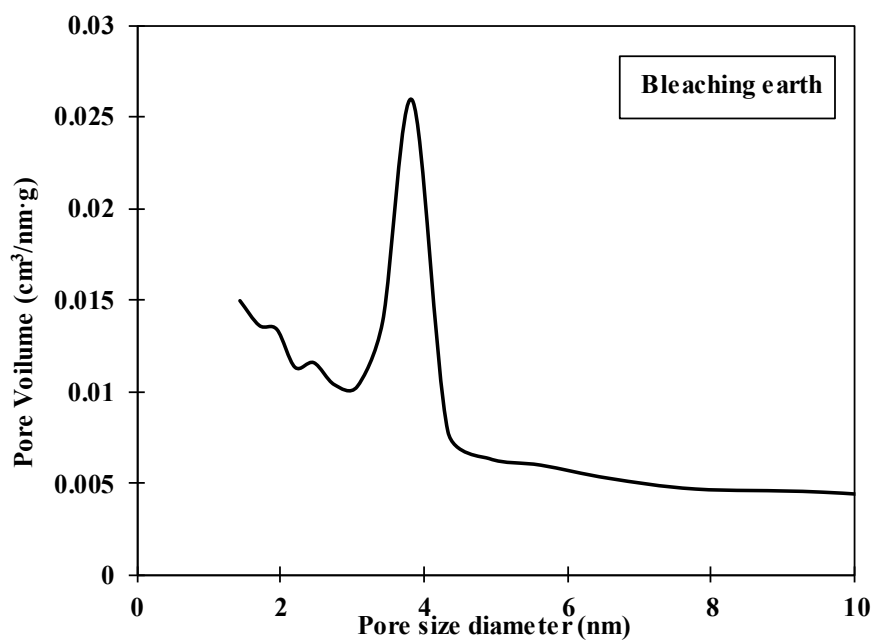


Figure A14 Pore size distribution of illite.



3872731635

CU Thesisis 6171022063 thesis / recv: 20072563 15:54:37 / seq: 19



**Figure A15** Pore size distribution of bleaching earth.

## Appendix B Relative crystallinity (%) calculation

From X-ray diffraction data; the intensity of the characteristic peaks at  $2\theta$  of 11.9, 15.7, 18.7, 20.4, 23.7, 27.1 and 31.4 of USY and modified USY is showed in Table B1. Total intensity of USY, USY-0.075, USY-0.15, and USY-0.3 is 446,273, 437,783, 399,822, and 354,453 respectively.

**Step 1:** Given the total intensity of USY is 100 %

**Thus;** The relative crystallinity =  $\frac{\text{Total Intensity of modified USY}}{\text{Total Intensity of parent USY}} \times 100 \%$

**Step 2:** Substituted in formula

$$\text{The relative crystallinity of USY-0.075} = \frac{437,783}{446,273} \times 100 \% = 98\%$$

$$\text{The relative crystallinity of USY-0.15} = \frac{399,822}{446,273} \times 100 \% = 91\%$$

$$\text{The relative crystallinity of USY-0.3} = \frac{354,453}{446,273} \times 100 \% = 81\%$$

**Table B1** Intensity of the characteristic peaks at  $2\theta$  of 11.9, 15.7, 18.7, 20.4, 23.7, 27.1 and 31.4 of USY and modified USY

| 2 $\theta$ | Intensity |           |          |         |
|------------|-----------|-----------|----------|---------|
|            | USY       | USY-0.075 | USY-0.15 | USY-0.3 |
| 11.9       | 56,571    | 57,214    | 55,286   | 47,500  |
| 15.7       | 100,988   | 94,500    | 95,286   | 83,929  |
| 18.7       | 47,500    | 46,461    | 41,500   | 36,500  |
| 20.4       | 54,750    | 54,000    | 48,500   | 44,214  |
| 23.7       | 85,714    | 81,429    | 73,250   | 66,000  |
| 27.1       | 55,250    | 55,429    | 46,500   | 41,429  |
| 31.4       | 45,500    | 48,750    | 39,500   | 34,881  |

## REFERENCES

- Auerbach, S., Carrado, K., and Dutta, P. (2003). Introduction to the structural chemistry of zeolites. *Handbook of zeolites and technology*, 74-95.
- Baerlocher, C., Meier, W.M., and Olson, D.H. (2001). IZA structure commission. Atlas of zeolite framework types, 46-65.
- Bendou, S. and Amrani, M. (2014). Effect of hydrochloric acid on the structural of sodic-bentonite clay. *Journal of Minerals and Materials Characterization and Engineering* 02, 404-413.
- Beyer, H.K. (2002). Dealumination techniques for zeolites. *Molecular Sieves Science and Technology* 3. 203-255
- Bergaya, F., Theng, B.K.G., and Lagaly, G. (2006). Modified clays and clay minerals. *Handbook of clay science*, 261-288.
- Cejka, J., Corma, A., and Zones, S. (2009). Morphological synthesis of zeolites. *Zeolites and catalysis: Synthesis reactions and applications* 1, 131-150.
- Chen, C.-w., Wu, W.-j., Zeng, X.-s., Jiang, Z.-h., and Shi, L. (2009). Study on several mesoporous materials catalysts applied to the removal of trace olefins from aromatics and commercial side stream tests. *Industrial & Engineering Chemistry Research* 40. 6646-6649.
- Dutta, D.K. (2018). Surface and Interface Chemistry of Clay Minerals, 289-329.
- Flanigen, E.M., Broach, R.W., Wilson, S.T., and Kulprathipanja S. (2010). Zeolite types and structures. *Zeolites in industrial separation and catalysis*, 27-55.
- Hino, M., Kurashige, M., Matsushashi, H., and Arata, K. (2006). The surface structure of sulfated zirconia: studies of XPS and thermal analysis. *Thermochimica Acta* 441, 35-41.
- Komadel, P. (2016). Acid activated clays: Materials in continuous demand. *Applied Clay Science* 131, 84-89.
- Li, G.-l., Luan, J.-n., zeng, X.-s. and Shi, L. (2011). Removal of trace olefins from aromatics over metal-halides-modified clay and its industrial test. *Industrial & Engineering Chemistry Research* 50, 6646-6649.
- Li, J., Liu, H., An, T., Yue, Y., and Bao, X. (2017). Carboxylic acids to butyl esters over dealuminated–realuminated beta zeolites for removing organic acids from bio-

- oils. RSC Advances 7, 33714-33725.
- Liu, N., Pu, X., Wang, X., and Shi, L. (2013). Study of alkylation on a Lewis and Brønsted acid hybrid catalyst and its industrial test. Industrial and Engineering Chemistry 20, 2848-2857
- Mukarakate, C., Zhang, X., Stanton, A.R., Robichaud, D.J., Ciesielski, P.N., Malhotra, K., Donohoe, B.S., Gjersing, E., Evans, R.J., Heroux, D.S., Richards, R., Iisa, K., and Nimlos, M.R. (2014). Real-time monitoring of the deactivation of HZSM-5 during upgrading of pine pyrolysis vapors. Green Chemistry 16, 1444-1461.
- Murray, H.H. (2006). Structure and composition of the clay minerals and their physical and chemical properties. Development in Clay Science, 7-31.
- Ouellette, R.J. and Rawn, J.D. (2014). Introduction to organic reaction mechanisms. Organic Chemistry 30, 75-110.
- Pettinari, C., Marchetti, F., and Martini, D. (2004). Metal complexes as hydrogenation catalysts. Comprehensive Coordination Chemistry II 9, 75-139.
- Pu, X., Liu, N.-w., Jiang, Z.-h., and Shi, L. (2012). Acidic and catalytic properties of modified clay for removing trace olefin from aromatics and its industrial test. Industrial & Engineering Chemistry Research 51, 13891-13896.
- Pu, X., Liu, N.-w., and Shi, L. (2015). Acid properties and catalysis of USY zeolite with different extra-framework aluminum concentration. Microporous and Mesoporous Materials 201, 17-23.
- Pu, X. and Shi, L. (2013). Commercial test of the catalyst for removal of trace olefins from aromatics and its mechanism. Catalysis Today 212, 115-119.
- Rabie, A.M., Mohammed, E.A., and Negm, N.A. (2018). Feasibility of modified bentonite as acidic heterogeneous catalyst in low temperature catalytic cracking process of biofuel production from nonedible vegetable oils. Journal of Molecular Liquids 254, 260-266.
- Sadeghbeigi, R. (2012). FCC feed characterization. Fluid catalytic cracking handbook, 51-86.
- Sidorenko, A.Y., Kravtsova, A.V., Aho, A., Heinmaa, I., Kuznetsova, T.F., Murzin, D.Y., and Agabekov, V.E. (2018). Catalytic isomerization of  $\alpha$ -pinene oxide in



- the presence of acid-modified clays. Molecular Catalysis 448, 18-29.
- Taylocra, R., Bo, M.L., Christian, G.D., and Jaromrir Ir. (1991). Bromine number determination by coulometric flow-injection titration. Talanta 39, 789-794.
- Tian, Y., Meng, X., and Shi, L. (2013). Synthesis of SO<sub>3</sub>H-functionalized ionic liquids and their novel application in removal of trace olefins from aromatics. Industrial & Engineering Chemistry Research 52, 6655-6611.
- Xin-Mei, L. and Zi-Feng, Y. (2001). Optimization of nanopores and acidity of USY zeolite by citric modification. Catalysis Today 68, 145-154.
- Yao, J., Liu, N., Shi, L., and Wang, X. (2015). Sulfated zirconia as a novel and recyclable catalyst for removal of olefins from aromatics. Catalysis Communications 66, 126-129
- Yan, Z., Ma, D., Zhuang, J., Liu, X., Liu, X., Han, X., Bao, X., Chang, F., Xu, L., and Liu, Z. (2003). On the acid-dealumination of USY zeolite: a solid state NMR investigation. Journal of Molecular Catalysis 194, 153-167.
- Yildiz, N., Aktas, Z., and Calimli, A. (2004). Sulphuric acid activation of a calcium bentonite. Particulate science and Technology 22, 21-33.
- Zhirong, L., Azhar Uddin, M., and Zhanxue, S. (2011). FT-IR and XRD analysis of natural Na-bentonite and Cu(II)-loaded Na-bentonite. Molecular and Biomolecular Spectroscopy 79, 1013-1016.

**VITA**

|                              |  |
|------------------------------|--|
| <b>NAME</b>                  | Mr. Sirawit Lertpraporn  |
| <b>DATE OF BIRTH</b>         | 28 Sep 1995  |
| <b>PLACE OF BIRTH</b>        | Bangkok, Thailand  |
| <b>INSTITUTIONS ATTENDED</b> | 2018-2020 Master Degree of Science in Petroleum and Petrochemical College Chulalongkorn University, Bangkok, Thailand<br>2014-2018 Bachelor Degree in Chemical Engineering, Faculty of Engineer, Kasetsart University, Bangkok, Thailand |
| <b>HOME ADDRESS</b>          | 27/7 moo5 siam natural home village Pantainorasingh Mueng Samut Sakon 74000  |